Supporting Information

Engineering fluorescent protein chromophore with internal reference for high-fidelity ratiometric G4 imaging in living cells

Jiao-Na Han, Caijun Zhong, Mingmin Ge, Shi Kuang* and Zhou Nie*

State Key Laboratory of Chemo/Biosensing and Chemometrics, College of Chemistry and Chemical Engineering, Hunan Provincial Key Laboratory of Biomacromolecular Chemical Biology, Hunan University, Changsha, 410082 (P. R. China)

*E-mail：niezhou.hnu@gmail.com; kuangshi@hnu.edu.cn

Table of Content

1. Experimental procedures

1.1 Materials and Equipment

Unless otherwise stated, all organic reagents were purchased from commercial suppliers and used without further purification. All starting materials involved in the synthesis were purchased from Bide Pharmatech unless otherwise specified. Anhydrous sodium sulfate, acetic acid, piperidine, extra dry DMF, ethanol, and deuterated reagents were purchased from Energy Chemical (Shanghai, China). Thioflavin T (ThT) was obtained from Sigma-Aldrich (St. Louis, MO, USA). Tris and KCl were purchased from Sangon Biotech (Shanghai, China). DMEM medium was purchased from Neuronbc (Beijing, China). DPBS and fetal bovine serum (FBS) were purchased from Biological Industries USA. CELLSAVING was purchased from New cell &Molecular Biotech (C40100). RNase A was obtained from Solarbio, USA. Lyso-Tracker Green and Mito-Tracker Green were purchased from Beyotime (China). The ultrapure water (18.2 MΩ·cm) used in the experiments was obtained from the Millipore Milli-Q system. Using tetramethylsilane (TMS) as an internal standard, ^{1}H NMR spectra were recorded at 400 MHz, and ^{13}C NMR spectra were recorded at 101 MHz. Chemical shifts (δ) were expressed in parts per million (ppm), and coupling constants (J) were expressed in Hertz (Hz). Silica gel plates were used for thin-layer chromatography, and silica gel (mesh 200-300) was used for column chromatography. Compounds were observed under UV light at 254 nm and 365 nm wavelengths. CD spectra and melting curves were measured at room temperature (RT) and variable temperature on a MOS-500 spectrophotometer (BioLogic, France). The pH measurements were performed on a Mettler-Toledo Delta 320 pH meter. All the stock solutions of the dyes were prepared in DMSO with a concentration of 5 mM and stored at -20 ℃. For the fluorescence experiments, the final concentration of dyes was adjusted to 1 μM (DMSO: buffer=1: 99). For direct visualization imaging experiments, the final concentration of the dye was adjusted to 5 μM (DMSO: buffer = 1: 99). In cell experiments, the dye was diluted to the indicated concentration as following: 5 μM (DMSO: buffer = 1: 99), 10 μM (DMSO: buffer = 1: 99), 15 μM (DMSO: buffer = 1: 99) or 20 μM (DMSO: buffer = 2: 98).

1.2 Oligonucleotides

Oligonucleotides were synthesized and purified by Sangon Biotech (Shanghai, China) (HPLC-purified sequences were shown in Table S1). Oligonucleotide stock solutions were prepared by directly dissolving oligonucleotides into their respective buffer solution and annealed in a thermal cycler. The oligonucleotides were heated at 90 °C for 5 min and then slowly cooled to 4 °C overnight before use.

1.3 Fluorescence Studies

Fluorescence experiments were performed on a QuantaMasterTM fluorescence spectrophotometer (PTI, Canada). Spectra were recorded at 2.5 nm excitation and emission slit widths using 2 mm × 10 mm path length quartz cuvettes unless otherwise stated. In titration experiments, a fixed concentration (1 μM) of probes was mixed with G4 oligonucleotides at different concentration (0-10 μM) in 100 mM KCl, and 25 mM Tris-HCl buffer, respectively. The mixtures were homogenized with a mixer at RT, then excitation and emission spectra were recorded.

1.4 UV-Vis Absorption Studies

UV-Vis absorption spectra were recorded on a UV-Vis spectrophotometer (Agilent) using a 10 mm optical-length quartz cuvette. A fixed concentration (5 μM) of dyes was mixed with a 5-fold amount of G4 oligonucleotide in 100 mM KCl, 25 mM Tris-HCl buffer at pH = 7.4. After mixing with a mixer at RT, the UV-Vis spectra of the probe-oligonucleotide complexes were measured in the 400–800 nm range.

1.5 Binding Affinity Measurements

The dissociation constant (K_d) values of the probe-G4 complexes were determined by measuring the fluorescence intensity at a fixed concentration (1.0 μM) of probes with increased G4 concentration. Then use the S1 equation[1] to perform nonlinear regression fitting on the data to obtain the K_d values.

$$Y = Y_{max}X/ (K_d + X) \quad (S1)$$

This equation assumed a 1:1 binding of the probe with G4, where Y represents the fold change in the fluorescence enhancement of the probe, Y_{max} represents the fold change in the fluorescence enhancement of the probe when saturated with G4, and X is the concentration of G4. The final data analysis was performed using Origin 2021.

1.6 Calculation of Fluorescence Quantum Yield

The quantum yield was calculated using Equation S2[2]

$$\Phi_{F(X)} = \Phi_{F(S)} (n_X / n_S)^2 A_S F_X / (A_X F_S) \quad (S2)$$

where Φ is the fluorescence quantum yield, A is the absorbance at the excitation wavelength, F is the area under the corrected emission curve, and n is the refractive index of the solvent. The subscripts S and X represent standard and unknown, respectively. The absorbances of the probes and Rhodamine 6G standard were kept below 0.05.

1.7 Circular Dichroism (CD) Spectroscopy

Circular dichroism (CD) spectra were measured on a MOS-500 spectrophotometer (BioLogic, France) and a temperature-controlled circulator. Before measurement, oligonucleotides were mixed with reaction buffer and annealed, and all samples were measured three times in the wavelength range of 240–360 nm at a scan rate of 100 nm/min, with a slit of 5 nm, and all CD spectra were collected. The quartz cuvette of 10 mm path length was used in all experiments. In the CD melting experiment, the temperature range of the melting curve was 25-95 °C, the interval was 1 °C, and the stabilization time was 1 min.

1.8 Photo-bleaching Analysis

Water droplets of NHCouI-NG16 complex (1 μM) and mCherry (1 μM) were formed in the presence of mineral oil. Photobleaching experiments were performed with a 20 mW solid-state laser for 30 min under a Nikon confocal microscope. Fluorescence images were captured every 8 s with a camera through a 10 X objective, and ROI analysis was performed with the NIS element viewer.

1.9 Direct two-color visualization

Direct two-color visualization of NHCouI-oligonucleotide complexes was performed using IVIS Lumina XR (IS1241N6071). The excitation and emission channels for GFP and DsRed were used, respectively. Fluorescence imaging of NHCouI-G4 complexes was recorded through the corresponding excitation and emission channels (GFP and DsRed channel, respectively). We calculated the signal-to-background ratios (S) using the equation:

$$S = (F-F_0)/F_0 \quad (S3)$$

Where F is the fluorescence intensity of corresponding NHCouI-oligonucleotide complexes, and F_0 is the fluorescence intensity of the Tris-HCl buffer. GFP channel: E_x/E_m 480/500-550 nm; DsRed channel: E_x/E_m 530/ 550-620nm

1.10 DFT Calculations.

Investigating the fluorescence properties of NMNaI, NECouI, and NHCouI in water, density functional theory (DFT) was performed using Gaussian 09. All of the molecules in the ground state (S0) and excited state (S1) setting the 6-31+G(d) group in water were geometrically optimized, using density functional theory calculations at the B3LYP level. The HOMO and LUMO energies of the S0 and S1 states were calculated from the geometrically optimized NMNaI, NECouI, and NHCouI.

1.11Molecular Modeling

The crystal structure of G-quadruplex NG16 was downloaded from the RCSB protein database (PDB code: 2LXV)[3, 4]. 2LXV is a dimer, and only the first chain is used. The probe NHCouI was optimized by Gaussian 09 using DFT calculations. NHCouI and NG16 were prepared by AutoDockTools, and docking simulation was performed by AutoDock 4.2.6 to study the interaction between molecules.[5] The binding mode of NHCouI to this antiparallel G4 TBA (PDB code: 2GKU)[6] and hybrid parallel G4 HT (PDB code: 2GKU)[7] was investigated using the same method as 2LXV. In this paper, the docking model with the lowest free energy was selected for further research. All graphics were rendered using the Discovery Studio 2016 Client program.

1.12 Calculation of octanol−water partition coefficients

The octanol−water partition coefficients were calculated using Equation S[8]

$$\log P = \log (c_{oct}/c_w) = \log (A_{oct}\varepsilon_w/A_w\varepsilon_{oct}) \quad (S4)$$

where c_{oct} and c_w are the probe concentration at equilibrium between the n-octanol and water phases, respectively. A_{oct} and A_w represent UV-Vis absorption of the probe at equilibrium between the n-octanol and water phases. ε_{oct} and ε_w represent the molar extinction coefficient of the probe at equilibrium between the n-octanol and water phases, respectively. The absorbance of the probes of known concentration was kept around 0.1.

1.13 Cytotoxicity Assay

Cytotoxicity of NHCouI was detected by CCK8. In a 96-well plate, 100 μL of the cell-containing solution was added to each well at a cell density of 2×10^4 cells and incubated at 37 C for 24 h. Then, the cells were treated with different NHCouI concentration (0, 0.1, 0.5, 1, 5, 10 μM) for 2 h, and 5 μM NHCouI for increasing the incubation time (0, 2, 4, 6, 8, 12, 24 h), respectively. After washing with PBS, cells were incubated with a mixture of 10 μL CCK8 and 90 μL DMEM for 4 h. The absorbance of the final solution at 450 nm was measured using a microplate reader (Biotek). The calculation formula of cell

viability (%): viability = (mean Abs. of treatment wells/mean Abs. of control wells) ×100%. Each experiment was replicated five times.

1.14 Flow cytometry

HeLa cells (2×10^5) incubated with or without cisplatin (12.5 μM) or erastin (10 μM) for 12 h in an incubator (Thermo Scientific) at 37 °C, with 5% CO_2 and 90% relative humidity, separately. After that, HeLa cells (2×10^5) suspensions were prepared in a cell separation buffer. Then, the cell suspensions were washed with PBS, followed by centrifugation (1000 rpm). 50 ug/mL Propidium Iodide (PI) was mixed with the cell suspensions for 30 min at 37°C. Then Flow cytometry analysis was performed using a flow cytometer (Abcam, USA).

1.15 Cell Culture and Imaging

HeLa cells were cultured in high glucose DMEM containing 10% fetal bovine serum (FBS), 100 U/mL penicillin, and 100 μg/mL streptomycin in an incubator (Thermo Scientific) at 37°C, with 5% CO2 and 90% relative humidity. HeLa cells (10^5) were cultured in 35 mm confocal culture dishes and incubated in an incubator for 12 h. Then HeLa cells were incubated with 5 μM, 10 μM, 15 μM, 20 μM NHCouI at 37°C for 2 h, respectively. Then washed with PBS three times, and used for imaging. Besides, 5 μM, 10 μM, 15 μM, 20 μM ThT was added to the confocal dishes plated with HeLa cells, incubated at 37°C for 2 h, washed with PBS three times, then the nuclei were counterstained with Hoechst 33342 for 30 min, washed with PBS three times, and used for imaging.

For the colocalization experiment, the confocal dishes plated with HeLa cells were incubated with Lyso-Tracker Green/Lyso-Tracker Red and Mito-Tracker Green/Mito-Tracker Red (100 nM), respectively. Then the dishes were washed three times with PBS, then incubated with 5 μM NHCouI or NHCou (containing 1% DMSO) for 2 h, and washed three times with PBS for imaging. Live cell imaging was performed using a Nikon confocal laser scanning microscope with a 60x oil immersion objective (Olympus, Melville, NY, model number: Ti-E+A1 MP) at room temperature. The cell-imaging fluorescence intensity generated on the cells was analyzed and quantified using ImageJ.

For drug-induced apoptosis and ferroptosis experiment, the confocal dishes plated with HeLa cells were incubated without or with cisplatin (12.5 μM) to induce apoptosis for 24 h or erastin (10 μM) to induce ferroptosis for 12 h at 37°C, respectively, and washed with PBS three times. Then the confocal dishes plated with HeLa cells were stained with NHCouI (5 μM NHCouI (containing 1% DMSO) at 37°C for 2 hours, washed three times with PBS, and used for imaging.

Cell fixation and imaging: HeLa Cells (10^5) were cultured in 35 mm confocal culture dishes and fixed with 4% paraformaldehyde for 20 min at 4 °C, then washed three times with DPBS, and permeabilized with 0.2% Triton X-100 in DEPC-PBS for 12 min at room temperature, then washed three times with DPBS. For enzymatic treatment experiments, the membrane permeabilized samples were incubated with 200 U/mL RNase A at 37°C for 4 hours, washed three times with PBS, and then incubated with 5 μM NHCouI (containing 1% DMSO) for 2 hours at 37°C, which was used directly for imaging after washing three times with PBS. For the competition experiment, the membrane permeabilized sample was incubated with 5 μM NHCouI (containing 1% DMSO) at 37°C for 2 hours and washed three times with PBS. Then 25 μM TMPyP4 was added and incubated at 37°C for 1 hour, washed three times with PBS, then used for imaging. For urea treatment experiments, the membrane permeabilized samples were incubated with 5 μM NHCouI (containing 1% DMSO) for 2 h, washed three times with PBS, and incubated with 7 M urea solution for 10 min for imaging. The urea was rinsed with PBS buffer for

imaging.

For the immunofluorescence experiment, the membrane permeabilized HeLa cells were incubated with 200 U/mL RNase A at 37°C for 4 hours, and washed three times with PBS. Cells were blocked with 20% goat serum, and incubated at 37°C for 1 h, washed three times with PBS. Then incubated with 1 μM BG4 antibody against G-quadruplexes at 37°C for 1 h, and washed three times with PBS.. Next, cells were incubated with anti-FLAG antibody (#8146) overnight at 4°C, stained with Alexa Fluor 647-labeled secondary antibody at 37°C for 1 hour, and washed three times with PBS. Then cells were stained with NHCouI (5 μM NHCouI (containing 1% DMSO) at 37°C for 2 hours, and washed three times with PBS.

For TUNEL assay to evaluate DNA fragmentation in cells, firsty, the confocal dishes plated with HeLa cells were incubated without or with cisplatin (12.5 μM) to induce apoptosis for 24 h or erastin (10 μM) to induce ferroptosis for 12 h at 37°C, respectively, and washed with PBS three times. Besides, the confocal dishes plated with HeLa cells were incubated with DNase I (40 U)at 37°C for 2 hours as a positive control group, and washed with PBS three times. Then, HeLa cells were fixed with 4% paraformaldehyde for 20 min at 4 °C, then washed three times with PBS, and permeabilized with 0.3% Triton X-100 in PBS for 5 min at room temperature, then washed three times with PBS. Next, the membrane permeabilized HeLa cells were incubated with the mixture of 45 μl of FITC fluorescent labeling solution and 5 μl of TdT enzyme at 37°C for 1 hours, then washed three times with PBS, and used for imaging. Fluorescence images were acquired on a Nikon confocal microscope 60 X oil immersion objective. Excitation wavelength and emission filters: NHCouI: Ex/Em = 405/500-550 nm; Ex/Em = 561/570-620 nm. Lyso-Tracker Green/Mito-Tracker Green/ThT: Ex/Em = 488/500-550 nm. Hoechst 33342: Ex/Em = 405/420-470 nm. NHCou: Ex/Em = 405/500-550 nm. Lyso-Tracker Red/ Mito-Tracker Red: Ex/Em = 561/570-620 nm. Alexa Fluor 647/Mito-Tracker Deep Red: Ex/Em = 640/663-738 nm. FITC: Ex/Em = 488/515-550 nm.

2. Synthesis and Characterization

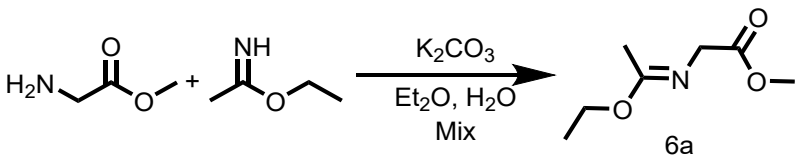

Synthesis of methyl (E)-2-((1-ethoxyethylidene)amino)acetate (6a)

potassium carbonate (50 mmol, 6.91 g) and methyl 2-aminoacetate (50 mmol, 6.28 g) were dissolved in 125 mL of ether and 20 mL of water, then ethyl acetimidate hydrochloride (50 mmol, 6.18 g) was added, and mixed well, and the mixture was shaken for 6 min. The ether was decanted, and 75 mL diethyl ether was added to the reaction solution, followed by shaking for 6 min, and the ether was decanted. The organic phase was dried with anhydrous sodium sulfate. The crude product 6a was obtained by rotary evaporation and freeze-drying, which was directly used in the next step without purification.

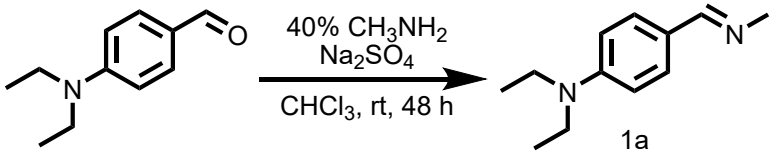

Synthesis of (E)-N, N-diethyl-4-((methylimino)methyl)aniline (1a)

To a stirred solution of 4-(diethylamino)benzaldehyde (20 mmol, 3.54 g), anhydrous sodium sulfate (20 g) in 100 mL of chloroform, 40% aqueous methylamine (256 mmol，5.0 mL） was added. After stirring at room temperature for 48 hours, the reaction solution was dried with anhydrous sodium sulfate and evaporated in vacuums to afford the crude product 1a, without purification and characterization for the next step.

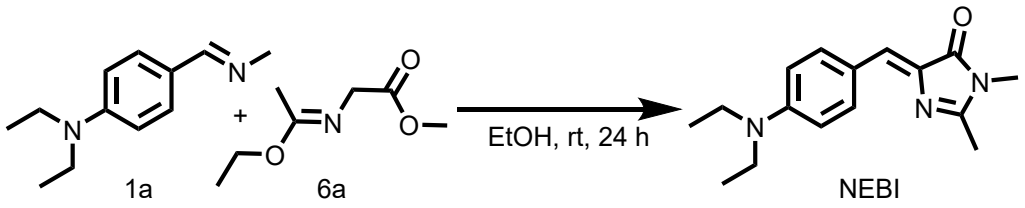

Synthesis of (Z)-5-(4-(diethylamino)benzylidene)-2,3-dimethyl-3,5-dihydro-4H-imidazo-4-one (NEBI)

Compound 1a (20 mmol, 3.54 g) was dissolved in 10 mL of ethanol, and compound 6a (50 mmol, 7.96 g) was slowly added dropwise to the reaction solution and stirred at room temperature for 24 hours. After the reaction, the reaction solution was cooled in ice water, and a yellow solid was precipitated, which was washed with cold ethanol (5 mL × 3) and ether (5 mL × 3). NEBI was obtained by freeze-drying (3.3 g, yield 61%). ^{1}H NMR (400 MHz, DMSO-d_6) δ 8.06 (d, J = 8.7 Hz, 2H), 6.87 (s, 1H), 6.73 (d, J = 8.8 Hz, 2H), 3.43 (q, J = 6.9 Hz, 4H), 3.10 (s, 3H), 2.33 (s, 3H), 1.14 (t, J = 7.0 Hz, 6H). ^{13}C NMR (101

MHz, DMSO-d_6) δ 170.09, 160.42, 149.24, 134.61, 126.94, 121.30, 111.52, 44.25, 26.59, 15.66, 12.96. MALDI-TOF MS *m*/*z* $[M + H]^+$ = calcd. for $C_{16}H_{22}N_3O$ 272.1757; found 272.1782.

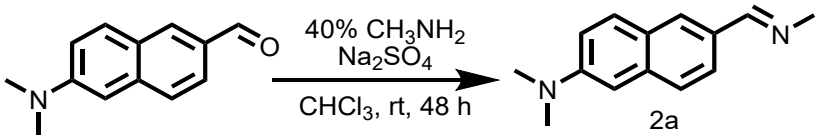

Synthesis of (E)-N, N-dimethyl-6-((methylimino)methyl)naphthalen-2-amine(2a)

6-(dimethylamino)-2-naphthaldehyde (5.0 mmol, 1.01 g) and anhydrous sodium sulfate (6 g) were added to 30 mL of chloroform, and then 40% aqueous methylamine (64 mmol, 1.26 mL) was added dropwise. After stirring at room temperature for 48 hours, the reaction solution was dried with anhydrous sodium sulfate and was removed by rotary evaporation. The crude product 2a was obtained by freeze-drying without purification for the next step.

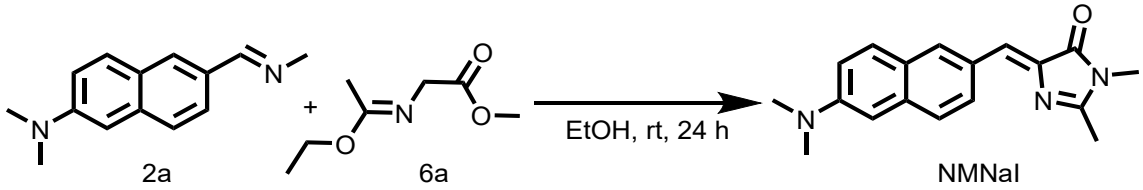

Synthesis of (Z)-5-((6-(dimethylamino)naphthalen-2-yl)methylene)-2,3-dimethyl -3,5-dihydro-4H-imidazol-4-one (NMNaI)

To a solution of compound 2a (5 mmol, 1.06 g) in 5 mL of ethanol, compound 6a (12.0 mmol, 2.38 g) was slowly added dropwise to the reaction solution and stirred at room temperature for 24 hours. After the reaction, the reaction solution was cooled in ice water; an orange-yellow solid was precipitated, washed with cold ethanol (5 mL × 3) and ether (5 mL × 3), and freeze-dried to obtain NMNaI (1.0 g, yield 68%). ^{1}H NMR (400 MHz, DMSO-d_6) δ 8.43 (d, J = 8.7 Hz, 1H), 8.36 (s, 1H), 7.78 (d, J = 9.1 Hz, 1H), 7.69 (d, J = 8.7 Hz, 1H), 7.26 (d, J = 9.1 Hz, 1H), 7.07 (s, 1H), 6.96 (s, 1H), 3.14 (s, 3H), 3.08 (s, 6H), 2.40 (s, 3H). ^{13}C NMR (101 MHz, DMSO-d_6) δ 170.28, 163.02, 150.03, 137.70, 135.92, 133.40, 130.18, 128.80, 128.04, 126.57, 126.27, 125.96, 116.72, 105.67, 26.71, 15.80. MALDI-TOF MS *m*/*z* $[M + H]^+$ = calcd. for $C_{18}H_{20}N_3O$ 294.1601; found 294.1580.

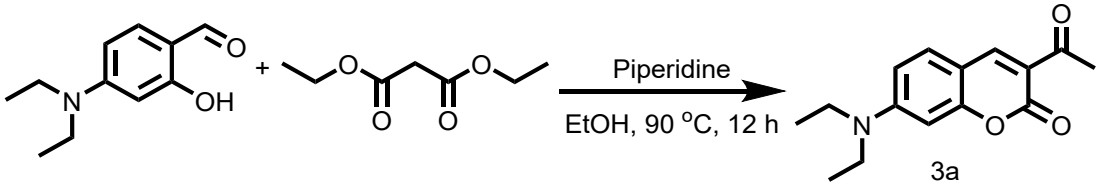

Synthesis of 3-acetyl-7-(diethylamino)-2H-chromen-2-one (3a)

A solution of 4-(diethylamino)-2-hydroxybenzaldehyde (19 mmol, 3.67 g), diethyl malonate (38 mmol, 6.08 g), and piperidine (38 mmol, 3.23 g) in 60 mL of ethanol, refluxed at 90 °C for 12 hours. The reaction progress was detected by TLC. After the reaction was completed, after cooling to room temperature, the reaction solution was rotary-evaporated, and the crude product 3a was freeze-dried and

directly used in the next step without purification.

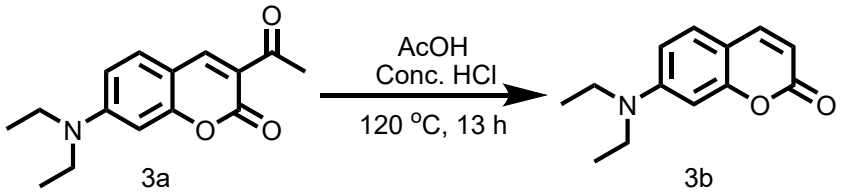

Synthesis of 7-(diethylamino)-2H-chromen-2-one (3b)

A solution of compound 3a (10 mmol, 2.59 g) in 20 mL of acetic acid and 20 mL of concentrated hydrochloric acid was refluxed at 120 °C for 13 hours. After the reaction solution was cooled to room temperature, the reaction solution was poured into 100 mL of ice water. Then 40% NaOH solution was added dropwise to the reaction mixture to adjust the pH to 5. A precipitate was precipitated in the reaction mixture, which was filtered, washed with water four times, and freeze-dried to obtain a brown solid 3b (1.84 g, yield 85%). ^{1}H NMR (400 MHz, DMSO-d_6) δ 7.84 ((d, J = 9.4 Hz, 1H), 7.44 (d, J = 8.7 Hz, 1H), 6.70 (d, J = 8.7 Hz, 1H), 6.53 (s, 1H), 6.01 (d, J = 9.2 Hz, 1H), 3.44 (q, J = 6.8 Hz, 4H), 1.14 (t, J = 6.8 Hz, 2H). ^{13}C NMR (101 MHz, DMSO-d_6) δ 161.44, 156.81, 150.95, 144.91, 129.75, 109.25, 108.65, 108.14, 97.10, 44.49, 12.77. MALDI-TOF MS m/z $[M + H]^+$ = calcd. For $C_{13}H_{16}NO_2$ 218.1176, found 218.1162.

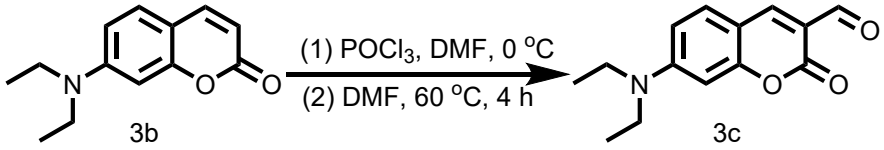

Synthesis of 7-(diethylamino)-2-oxo-2H-chromene-3-carbaldehyde (3c)

DMF (29.7 mmol, 2.31 mL) was added to a round-bottomed flask at 0 °C under an N_2 atmosphere, and phosphorus oxychloride (29.7 mmol, 3.63 mL) was slowly added dropwise to the reaction solution stirring for 1 hour. Then compound 3b (10 mmol, 2.17 g) was dissolved in 10 mL of DMF, then slowly added dropwise to the reaction solution, and refluxed at 60 °C for another 4 hours. After the reaction solution was cooled to room temperature, the reaction solution was added dropwise to 100 mL of ice water and stirred for 1 hour. Until the orange-yellow solid was precipitated, the precipitate was filtered, washed twice with water, then washed twice with diethyl ether. 3c was obtained after freeze-drying (1.96 g, 90% yield). ^{1}H NMR (400 MHz, DMSO-d_6) δ 9.92 (s, 1H), 8.43 (s, 1H), 7.70 (d, J = 8.9 Hz, 1H), 6.85 (d, J = 8.9 Hz, 1H), 6.63 (s, 1H), 3.54 (q, J = 6.6 Hz, 4H), 1.17 (t, J = 6.8 Hz, 6H). ^{13}C NMR (101 MHz, DMSO-d_6) δ 187.55, 161.15, 158.91, 153.90, 146.58, 133.51, 113.65, 110.93, 108.14, 96.85, 45.01, 12.82. MALDI-TOF MS m/z $[M + H]^+$ = calcd. for $C_{14}H_{16}NO_3$ 246.1125; found 246.1148.

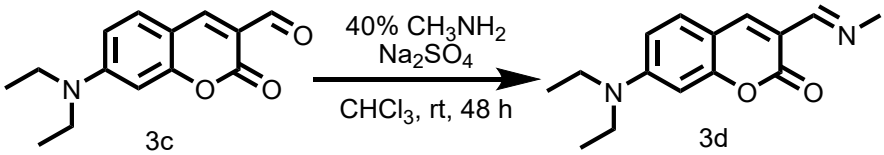

Synthesis of (E)-7-(diethylamino)-3-((methylimino)methyl)-2H-chromen-2-one (3d)

Compound 3c (2.5 mmol, 0.67 g) was dissolved in 15 mL of chloroform, then 40% methylamine aqueous solution (32 mmol, 0.63 mL) was added dropwise to the reaction solution, and the mixture was stirred at room temperature for 48 hours. After the reaction, the solution was dried with anhydrous sodium sulfate and removed by rotary evaporation. The crude product 3d was obtained by freeze-drying without purification for the next step.

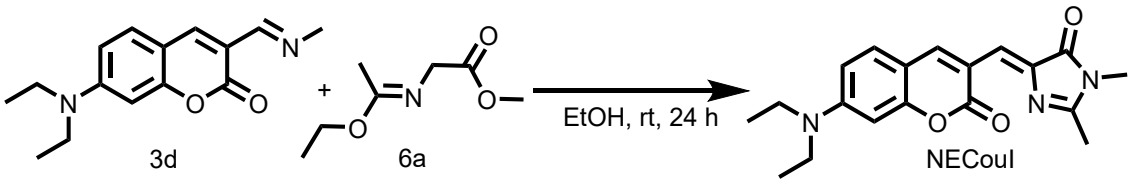

Synthesis of (Z)-5-((7-(diethylamino)-2-oxo-2H-chromen-3-yl)methylene)-2,3-dimethyl-3,5-dihydro-4H-imidazol-4-one (NECouI)

Compound 3d (3 mmol, 0.74 g) was dissolved in 6 mL of ethanol, and compound 6a (7.5 mmol, 1.19 g) was slowly added dropwise to the reaction solution and refluxed at room temperature for 24 hours. After the reaction was completed, the reaction solution was cooled to room temperature, ethyl acetate was added to the reaction solution, extracted with saturated sodium chloride, the organic phase was collected, dried over anhydrous sodium sulfate, rotary evaporated, and separated by silica gel column chromatography (DCM: EtOH = 150:1, v/v) to obtain the product NECouI (0.32 g, yield 32%). ^{1}H NMR (400 MHz, DMSO-d_6) δ 1H NMR (400 MHz, DMSO-d6) δ 9.18-8.98 (m, 1H), 7.51 (s, 1H), 7.07-7.00 (m, 1H), 6.74 (s, 1H), 6.56 (s, 1H), 3.74 (s, 3H), 3.40-3.30 (m, 4H), 2.36 (s, 3H), 1.16-1.10 (m, 6H). ^{13}C NMR (101 MHz, DMSO-d_6) δ 169.11, 162.99, 161.44, 156.82, 152.38, 146.05, 137.70, 131.63, 119.15, 113.18, 110.49, 109.18, 97.01, 52.97, 44.83, 41.64, 15.68, 12.87. MALDI-TOF MS *m*/*z* $[M + H]^+$ = calcd. for $C_{19}H_{22}N_3O_3$ 340.1656; found 340.1653.

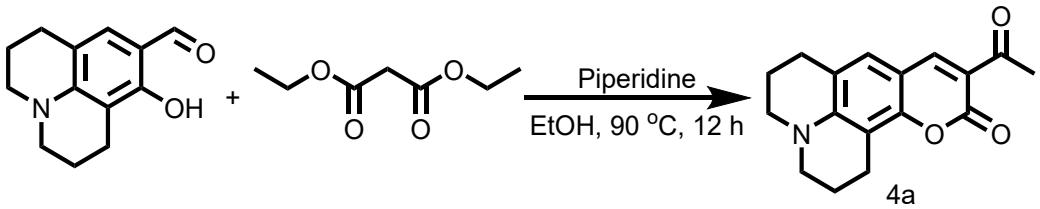

Synthesis of 10-acetyl-2,3,6,7-tetrahydro-1H,5H,11H-pyrano[2,3-*f*]pyrido[3,2,1-*ij*]quinolin-11-one (4a)

8-hydroxy-2,3,6,7-tetrahydro-1H,5H-pyrido[3,2,1-ij]quinoline-9-carbaldehyde (5 mmol, 1.08 g), diethyl malonate (10 mmol, 1.08 g) and piperidine (10 mmol, 0.85 g) were dissolved in 25 mL of ethanol and refluxed at 90 °C for 12 hours. TLC detected the reaction progress after the reaction was completed, cooling to room temperature. The reaction solution was rotary-evaporated, and the crude product 4a was freeze-dried and directly used in the next step without purification.

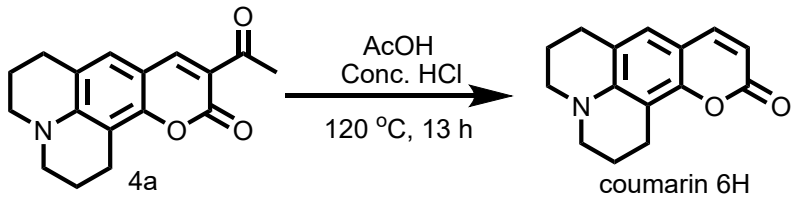

Synthesis of 2,3,6,7-tetrahydro-1H,5H,11H-pyrano[2,3-*f*]pyrido[3,2,1-*ij*]quin-olin-11-one (NHCou)

A solution of compound 3a (4 mmol, 1.13 g) in 10 mL of acetic acid and 10 mL of concentrated hydrochloric acid was refluxed at 120 °C for 13 hours. After the reaction was completed, after the reaction solution was cooled to room temperature, the reaction solution was poured into 50 mL of ice water. Then 40% NaOH solution was added dropwise to the reaction mixture to adjust the pH to 5. The precipitate was formed in the reaction mixture, which was filtered and washed with water four times. The brown solid coumarin 6H was obtained after lyophilization (0.77 g, 80% yield). ^{1}H NMR (400 MHz, DMSO-d_6) δ 7.72 (d, J = 8.2 Hz, 1H), 7.01 (s, 1H), 5.95 (d, J = 8.0 Hz, 1H), 3.26-3.23 (m, 4H), 2.75-2.69 (m, 4H), 1.91-1.86 (m, 4H). ^{13}C NMR (101 MHz, DMSO-d_6) δ 161.59, 151.65, 146.17, 145.09, 125.66, 118.42, 107.98, 107.79, 105.98, 49.73, 49.24, 27.28, 21.37, 20.50, 20.24. MALDI-TOF MS m/z $[M + H]^+$ = calcd. for $C_{15}H_{16}NO_2$ 242.1176; found 242.1201.

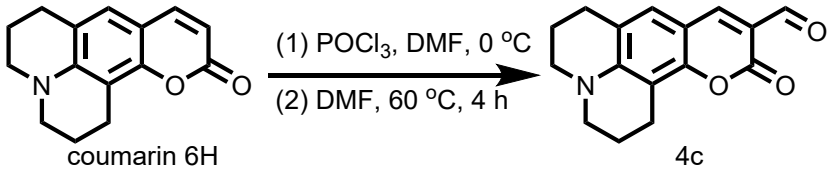

Synthesis of 11-oxo-2,3,6,7-tetrahydro-1H,5H,11H-pyrano[2,3-*f*]pyrido[3,2,1-*ij*]quinoline-10-carbaldehyde (4c)

Phosphorus oxychloride (9 mmol, 1.21 mL) was slowly added dropwise to the solution of DMF (9 mmol, 0.70 mL) at 0 °C under an N_2 atmosphere, and the reaction was stirred at 50 °C for 1 hour. Then compound NHCou (3 mmol, 0.72 g) was dissolved in 4 mL of DMF, then slowly added dropwise to the reaction solution, and refluxed at 60 °C for 4 hours. After the reaction solution was cooled to room temperature, the solution was added dropwise to 50 mL of ice water and stirred for 1 hour. After the brown solid was precipitated, filtering the crude product, then washed twice with water and then with ether, and lyophilized to obtain compound 4c (0.73 g, 92% yield). ^{1}H NMR (400 MHz, DMSO-d_6) δ 9.88 (s, 1H), 8.25 (s, 1H), 7.27 (s, 1H), 3.43-3.38 (m, 4H), 2.76-2.70 (m, 4H), 1.92-1.87 (m, 4H). ^{13}C NMR (101 MHz, DMSO-d_6) δ 187.38, 161.49, 153.67, 149.80, 145.86, 129.06, 120.28, 112.10, 107.91, 105.60, 50.29, 49.75, 27.15, 20.87, 19.92. MALDI-TOF MS m/z $[M + H]^+$ = calcd. for $C_{16}H_{16}NO_3$ 270.1125; found 270.1116.

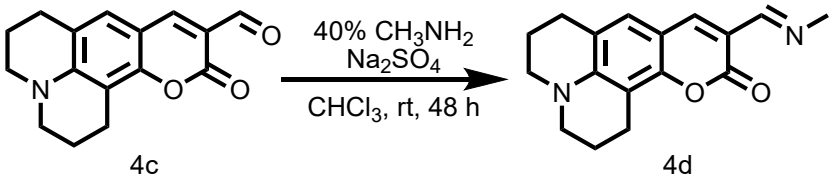

Synthesis of (E)-10-((methylimino)methyl)-2,3,6,7-tetrahydro-1H,5H,11H-Pyrano [2,3-f]pyrido[3,2,1-ij]quinolin-11-one (4d)

A solution of compound 4c (2.5 mmol, 0.67 g) and anhydrous sodium sulfate (3 g) in 15 mL of chloroform, 40% aqueous methylamine solution (32 mmol, 0.63 mL) were added dropwise to the reaction solution, and the mixture was stirred at room temperature for 48 hours. After the reaction, the solution was dried with anhydrous sodium sulfate and was removed by rotary evaporation. The crude product 4d was obtained by freeze-drying.

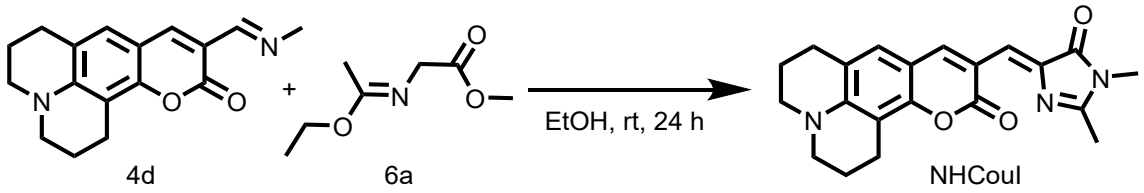

4d 6a NHCouI

Synthesis of (Z)-10-((1,2-dimethyl-5-oxo-1,5-dihydro-4H-imidazol-4-ylidene)meth-yl)-2,3,6,7-tetrahydro-1H,5H,11H-pyrano[2,3-f]pyrido[3,2,1-ij]quinolin-11-one (NHCouI)

Compound 4d (2.5 mmol, 0.71 g) was dissolved in 5 mL of ethanol, and compound 6a (6.3 mmol, 1.0 g) was slowly added dropwise to the reaction solution and stirred at room temperature for 24 hours. After the reaction was completed, ethyl acetate was added to the reaction solution and extracted with saturated sodium chloride. The organic phase was collected and dried over anhydrous sodium sulfate. The organic phase was rotary evaporated and separated by silica gel column chromatography (DCM: EtOH = 100:1) to obtain the product NHCouI (0.21 g, yield 27%). ^{1}H NMR (400 MHz, DMSO-d_6) δ 9.04 (s, 1H), 7.12 (s, 1H), 7.06 (s, 1H), 3.72 (s, 3H), 3.34-3.30 (m, 4H), 2.75-2.70 (m, 4H), 2.32 (s, 3H), 1.92-1.85 (m, 4H). ^{13}C NMR (101 MHz, DMSO-d6) δ 169.07, 162.26, 161.61, 151.64, 148.08, 146.03, 137.03, 127.40, 119.89, 119.64, 111.71, 108.96, 105.72, 52.98, 50.09, 49.53, 41.61, 27.10, 21.04, 19.97, 15.65. MALDI-TOF MS *m/z* $[M + H]^+$ = calcd. for $C_{21}H_{22}N_3O_3$ 364.1656; found 364.1644.

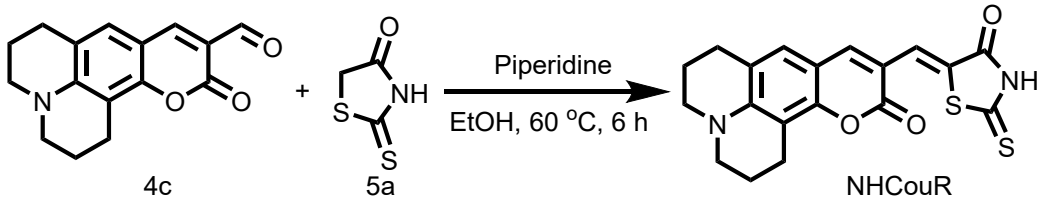

4c 5a NHCouR

Synthesis of (Z)-10-((4-oxo-2-thioxothiazolidin-5-ylidene)methyl)-2,3,6,7-tetrahydro-1H,5H,11H-pyrano[2,3-f]pyrido[3,2,1-ij]quinolin-11-one(NHCouR)

Compounds 4c (0.5 mmol, 0.13 g) and 5a (0.5 mmol, 0.067 g) were dissolved in 10 mL of ethanol solution, and then 100 μL of piperidine was added dropwise to stir at 60 °C for 6 hours. After the reaction was completed, the reaction solution was cooled to room temperature. Ethyl acetate was added to the solution and extracted with saturated sodium chloride. Then the organic phase was collected and dried over anhydrous sodium sulfate. The product NHCouR (0.12 g, 63% yield) was obtained by silica gel column chromatography (DCM: EtOH = 80:1) (0.12 g, 63% yield). ^{1}H NMR (400 MHz, DMSO-d_6) δ 13.51 (s, 1H), 7.91 (s, 1H), 7.43 (s, 1H), 7.18 (s, 1H), 3.83-3.79 (m, 2H), 3.50-3.47 (m, 2H), 2.74-2.70 (m, 4H), 1.93-1.88 (m, 4H). ^{13}C NMR (101 MHz, DMSO-d_6) δ 196.90, 186.94, 180.43, 160.80, 151.92, 148.68, 146.79, 128.52, 127.62, 120.11, 110.41, 109.00, 105.57, 50.20, 49.60, 26.02, 25.54, 23.81, 20.95,

19.92. MALDI-TOF MS *m/z* $[M + H]^+$ = calcd. for $C_{19}H_{16}N_2O_3S_2$ 385.0675; found 385.0688.

3. NMR spectra

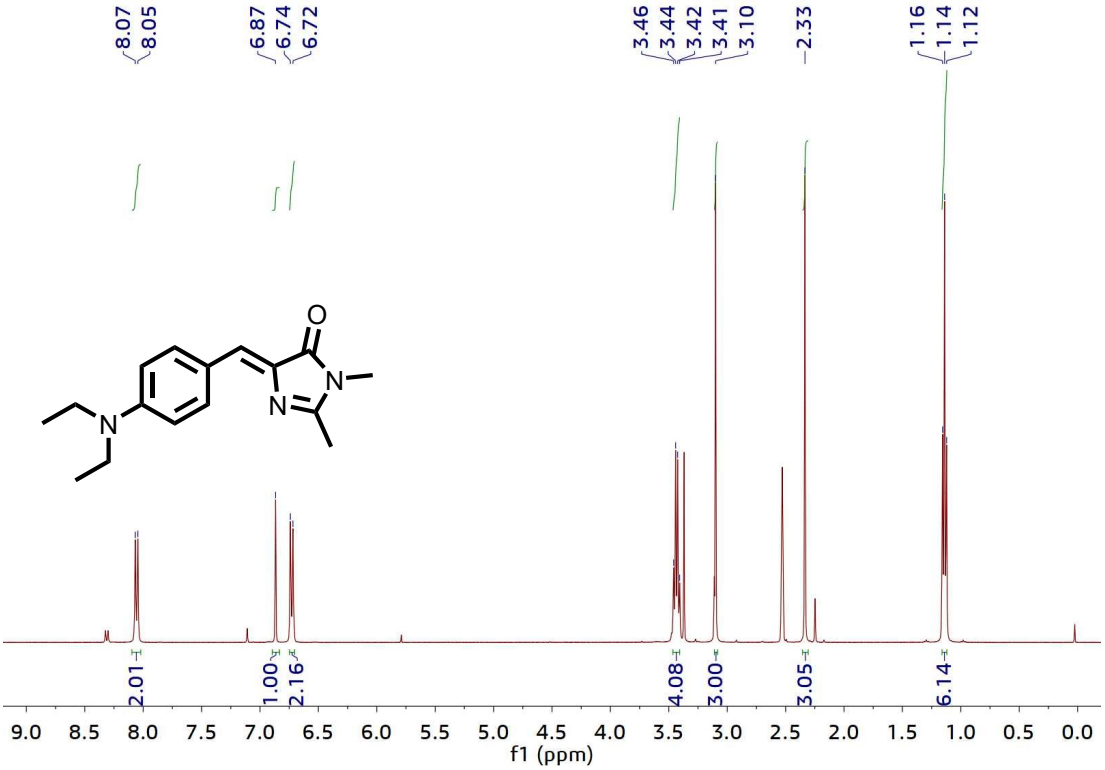

Fig. S1. ^{1}H NMR spectrum of NEBI in DMSO-d_6.

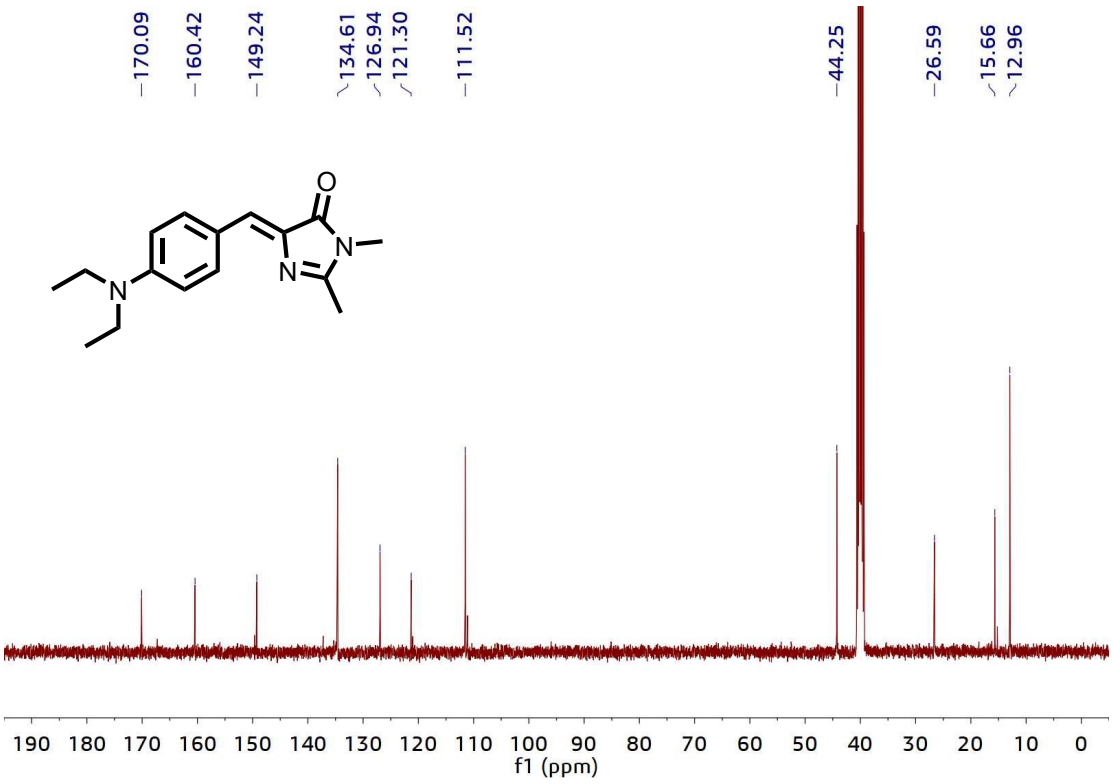

Fig. S2. ^{13}C NMR spectrum of NEBI in DMSO-d_6.

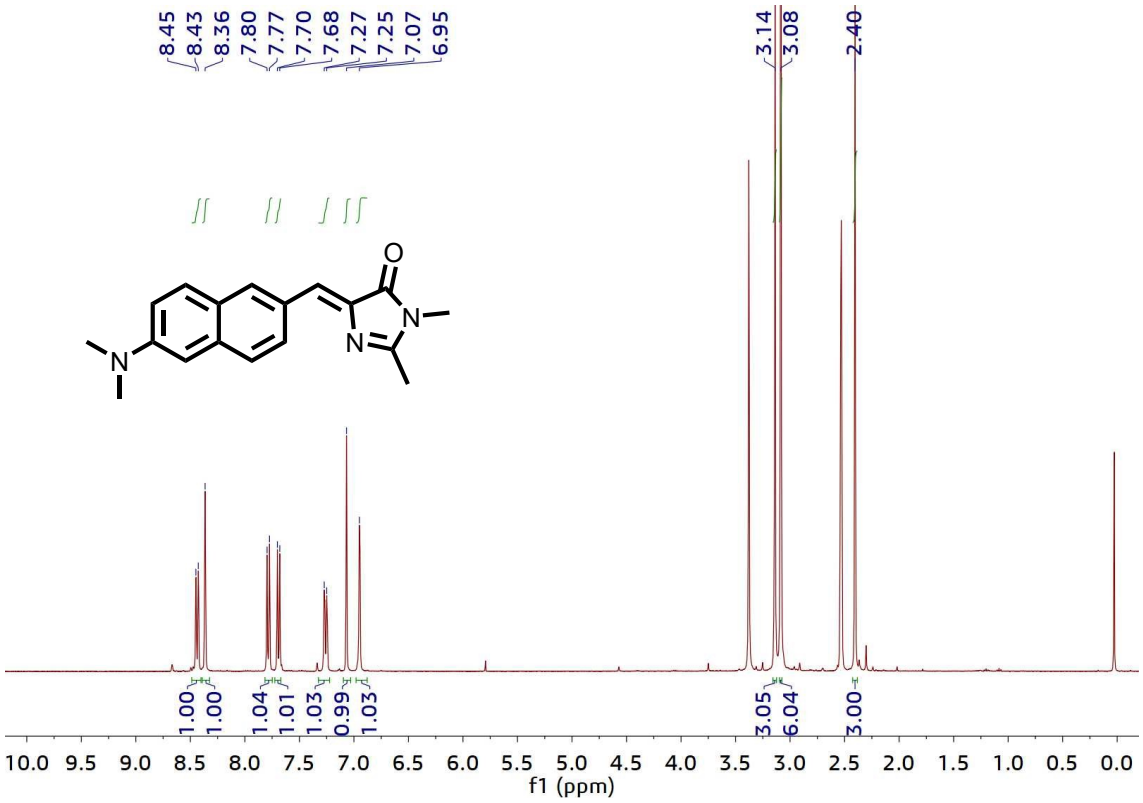

Fig. S3. ^{1}H NMR spectrum of NMNaI in DMSO-d_6.

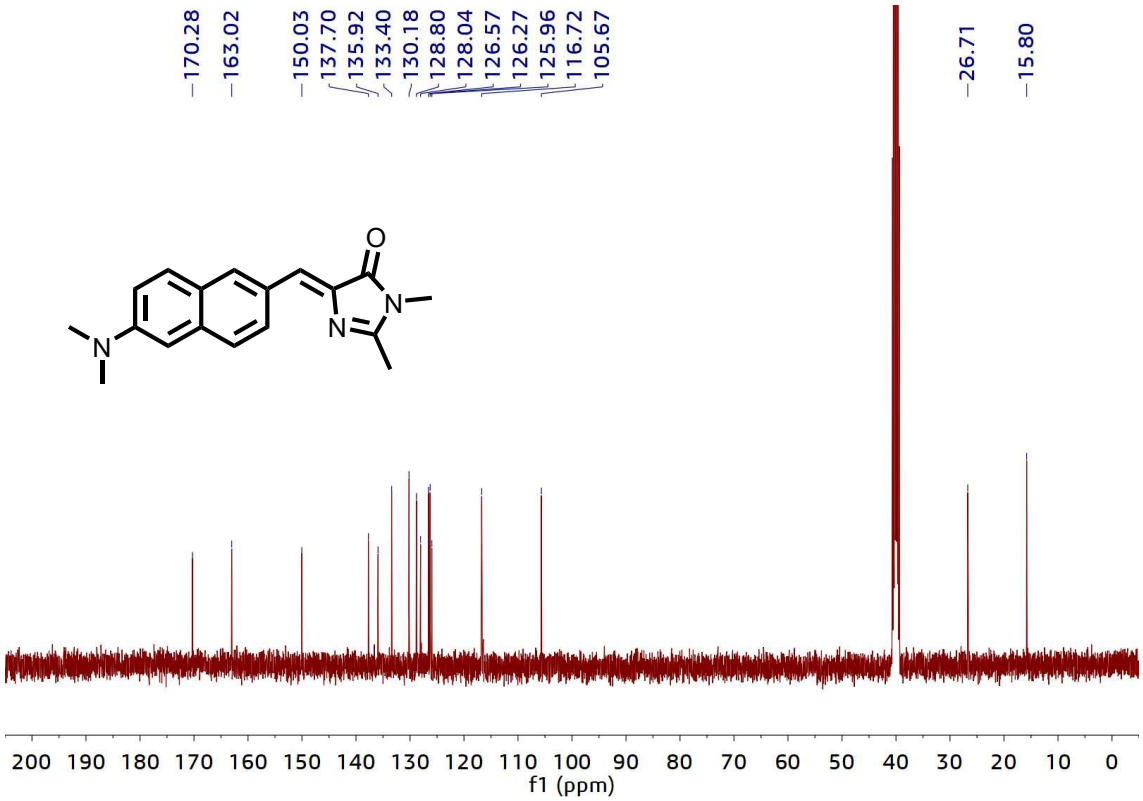

Fig. S4. ^{13}C NMR spectrum of NMNaI in DMSO-d_6.

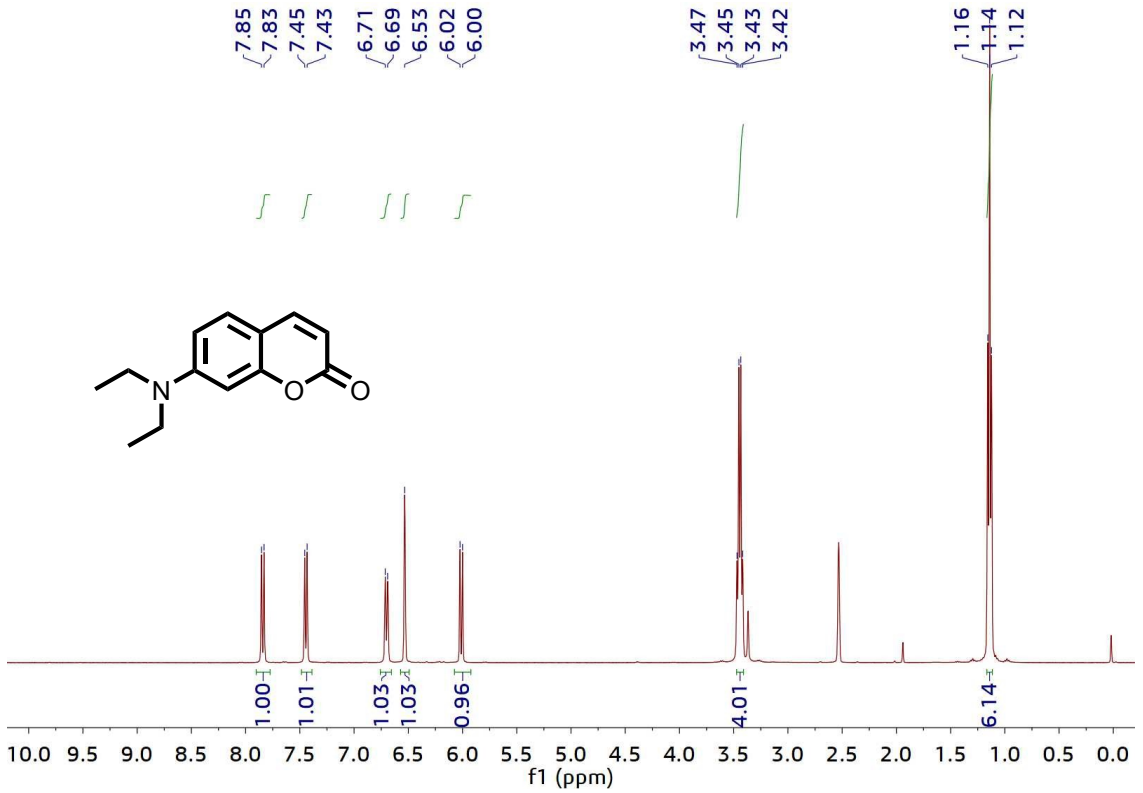

Fig. S5. ^{1}H NMR spectrum of 3b in DMSO-d_6.

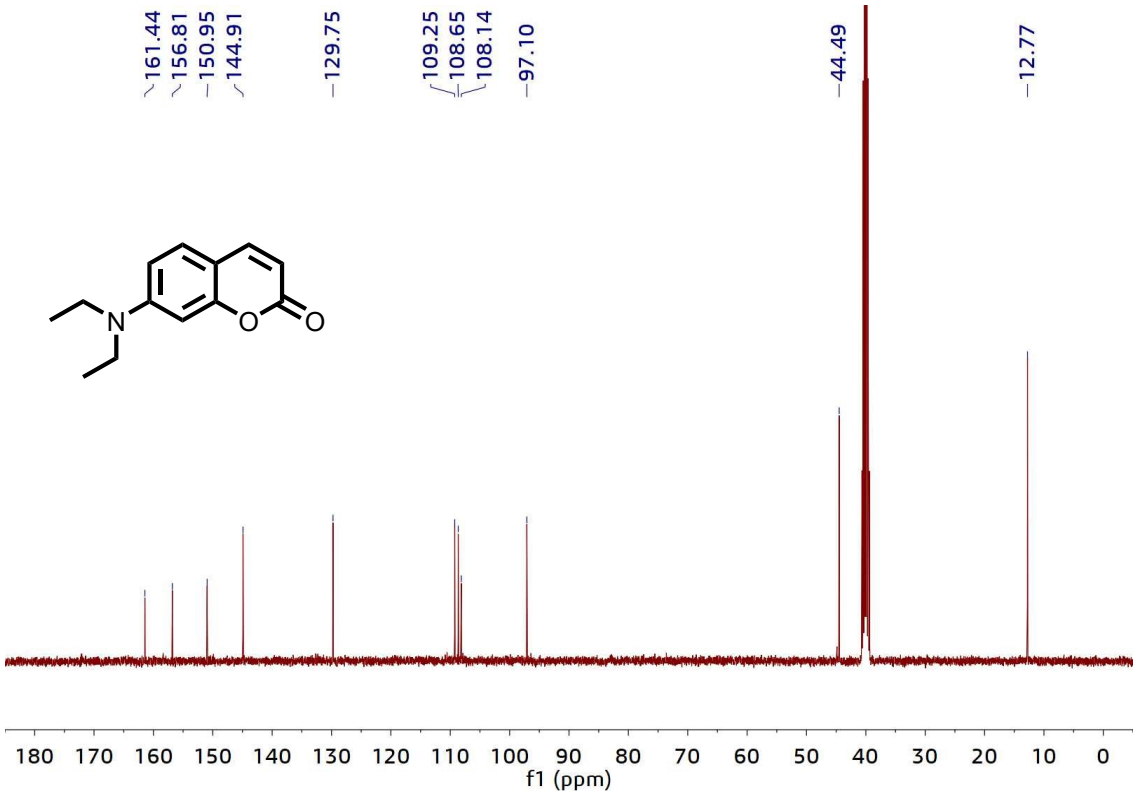

Fig. S6. ^{13}C NMR spectrum of 3b in DMSO-d_6.

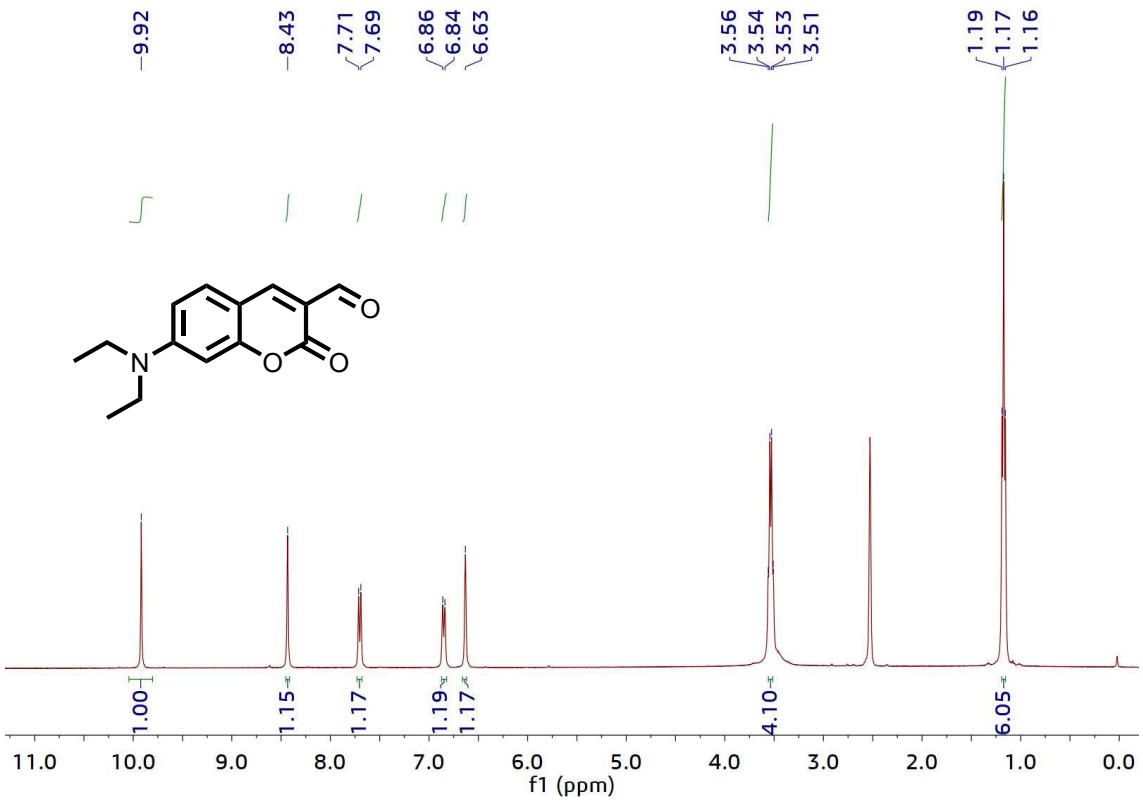

Fig. S7. ^{1}H NMR spectrum of 3c in DMSO-d_6.

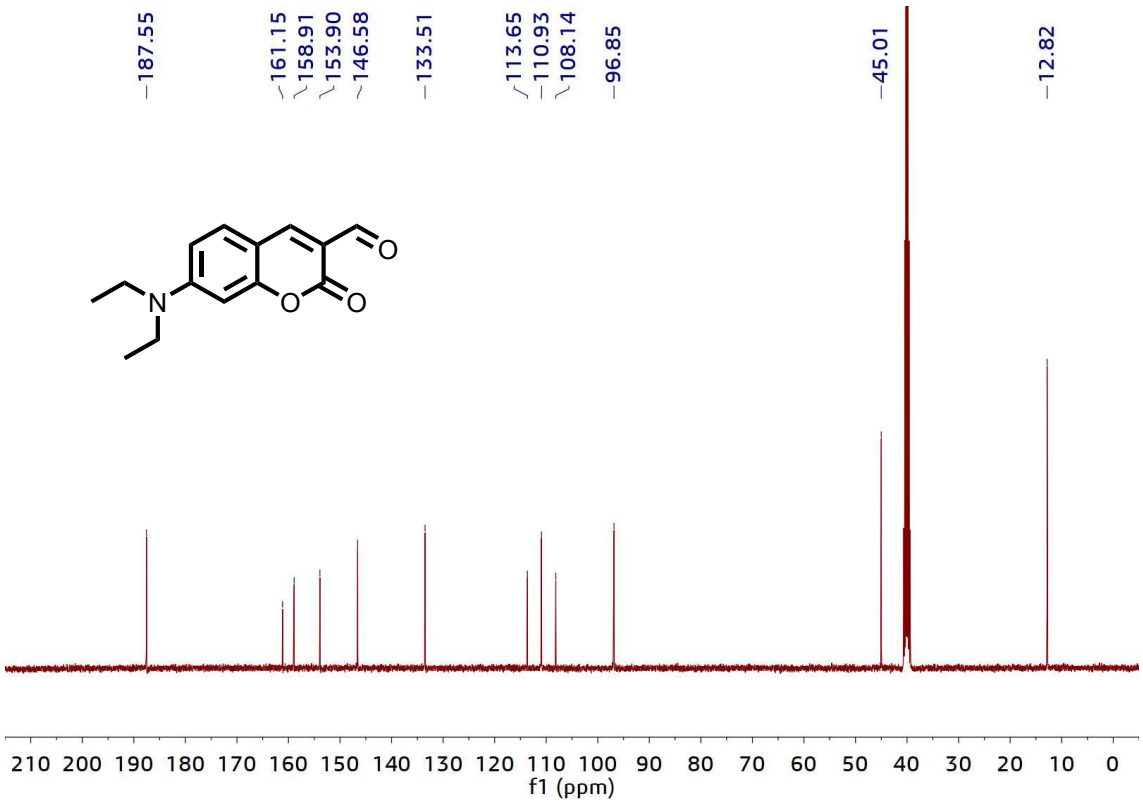

Fig. S8. ^{13}C NMR spectrum of 3c in DMSO-d_6.

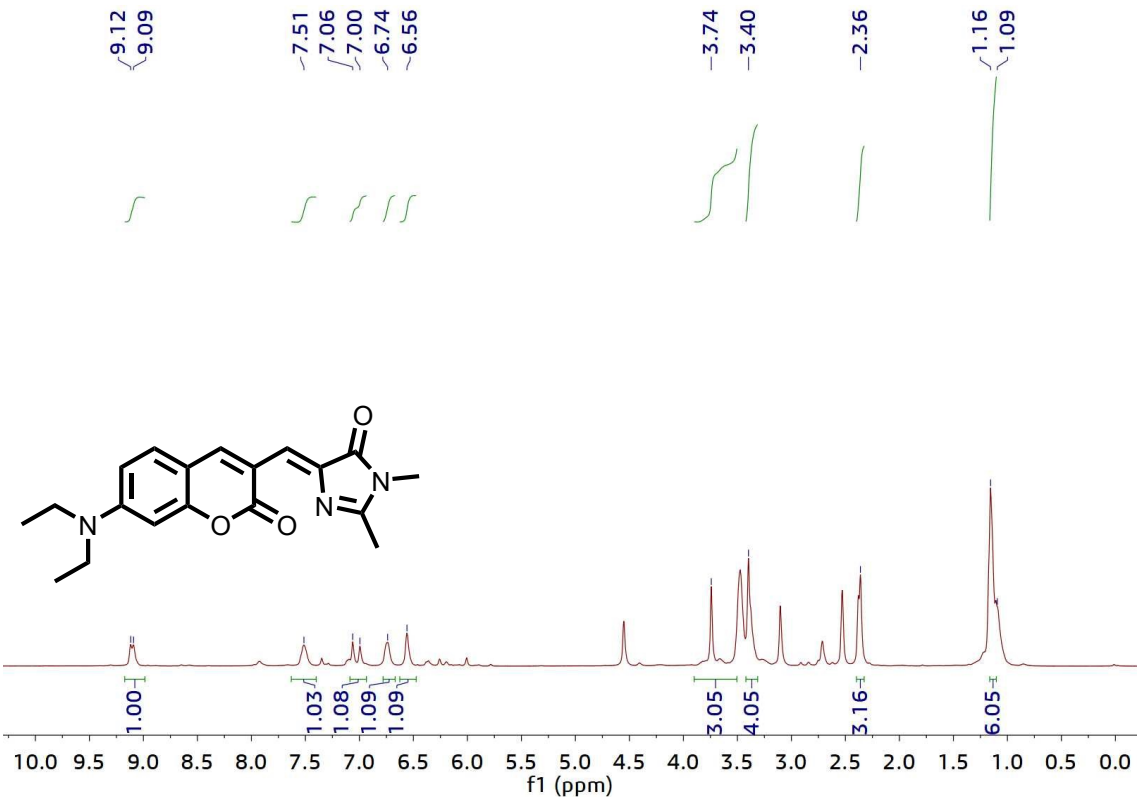

Fig. S9. ^{1}H NMR spectrum of NECouI in DMSO-d_6.

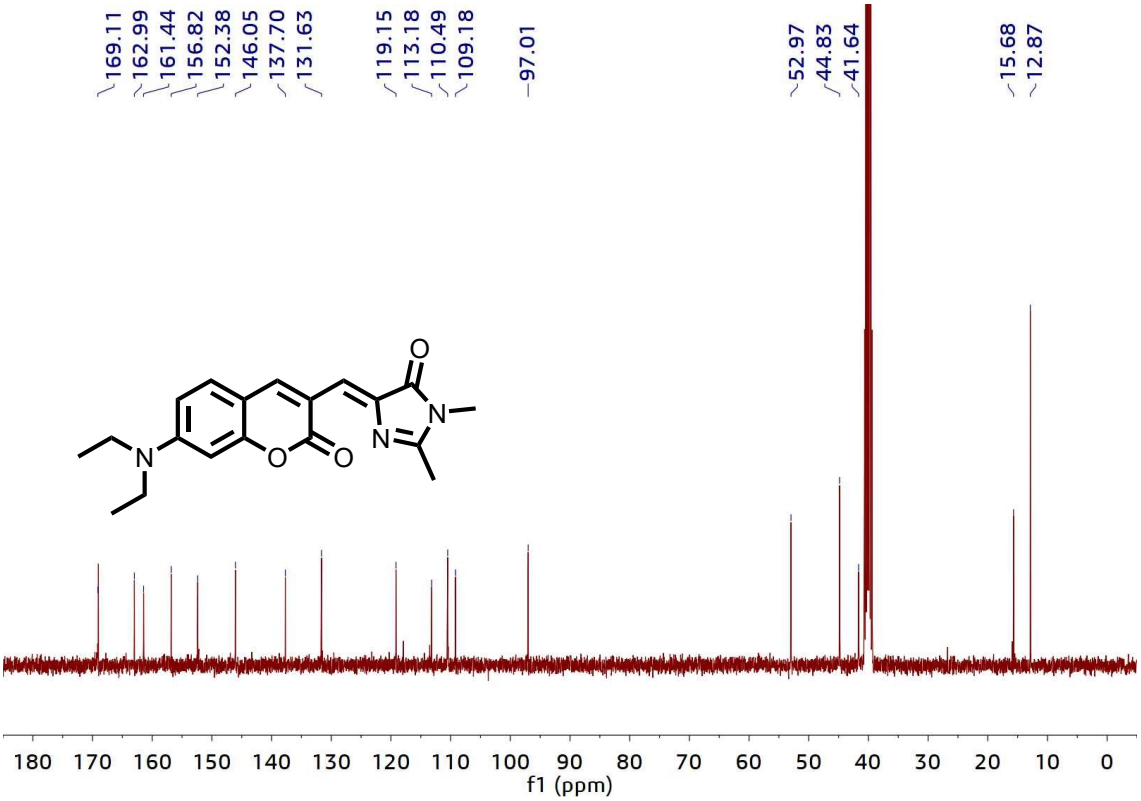

Fig. S10. ^{13}C NMR spectrum of NECouI in DMSO-d_6.

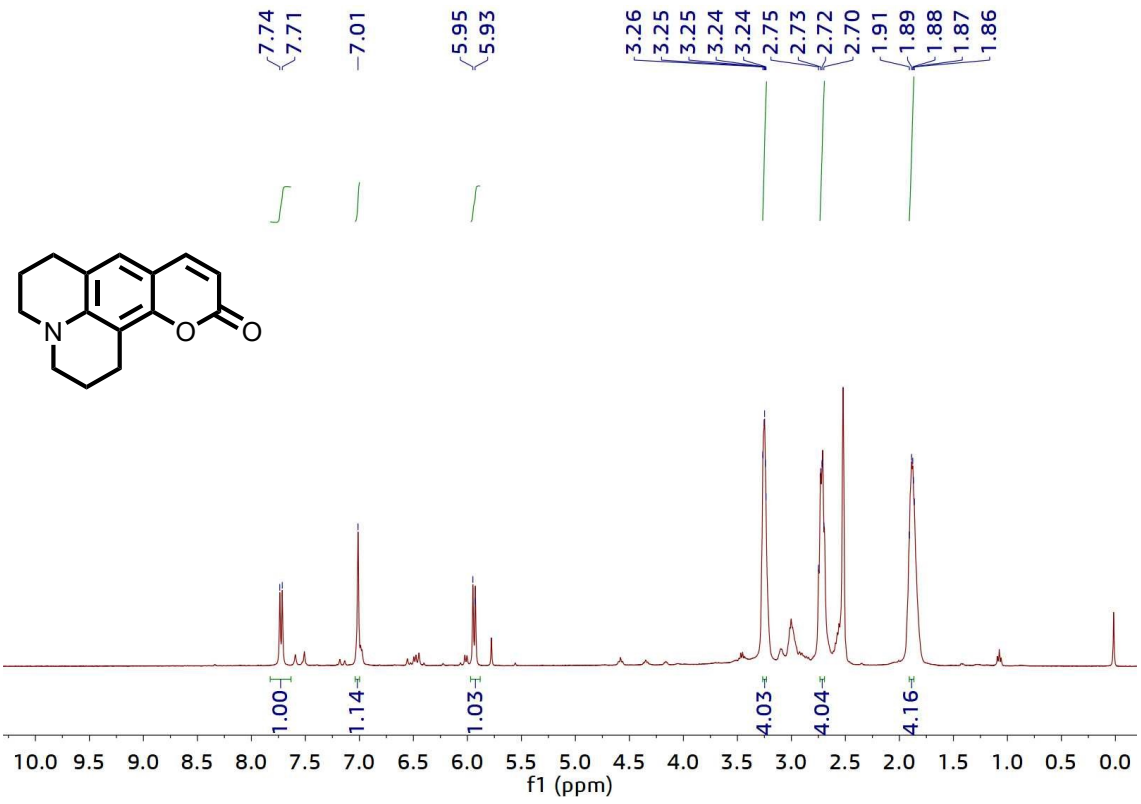

Fig. S11. ^{1}H NMR spectrum of NHCou in DMSO-d_6.

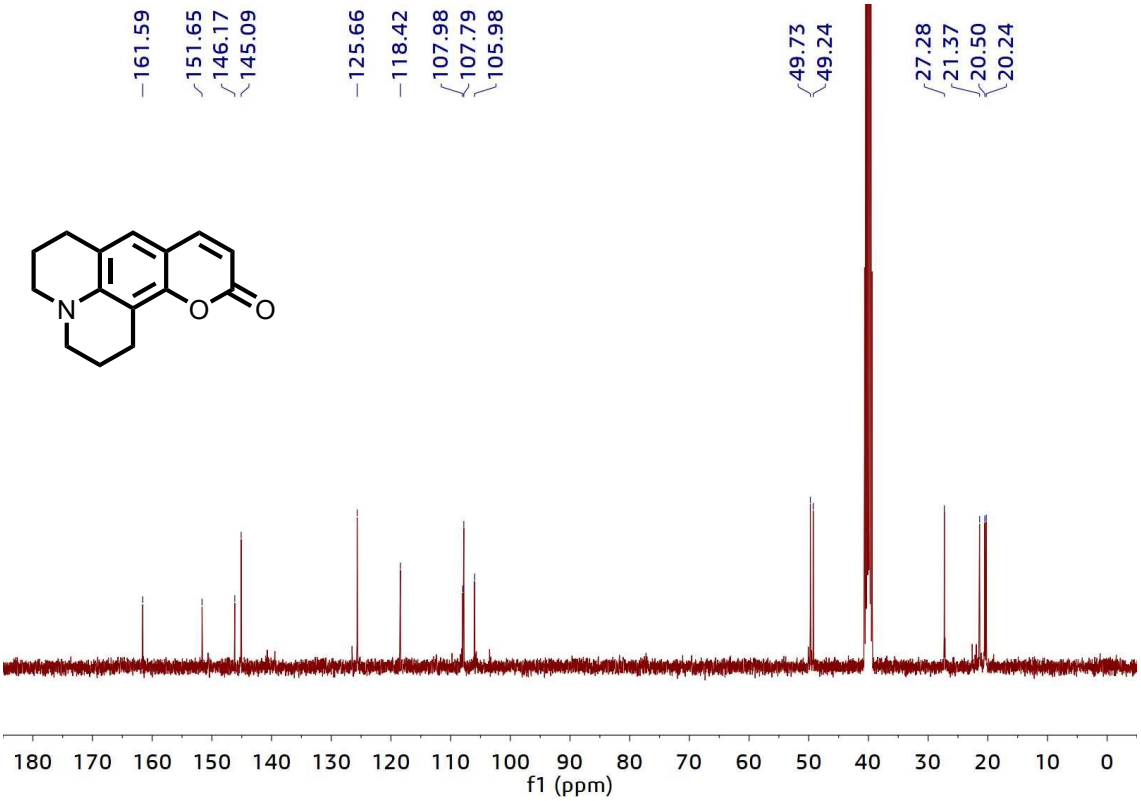

Fig. S12. ^{13}C NMR spectrum of coumarin 6H in DMSO-d_6.

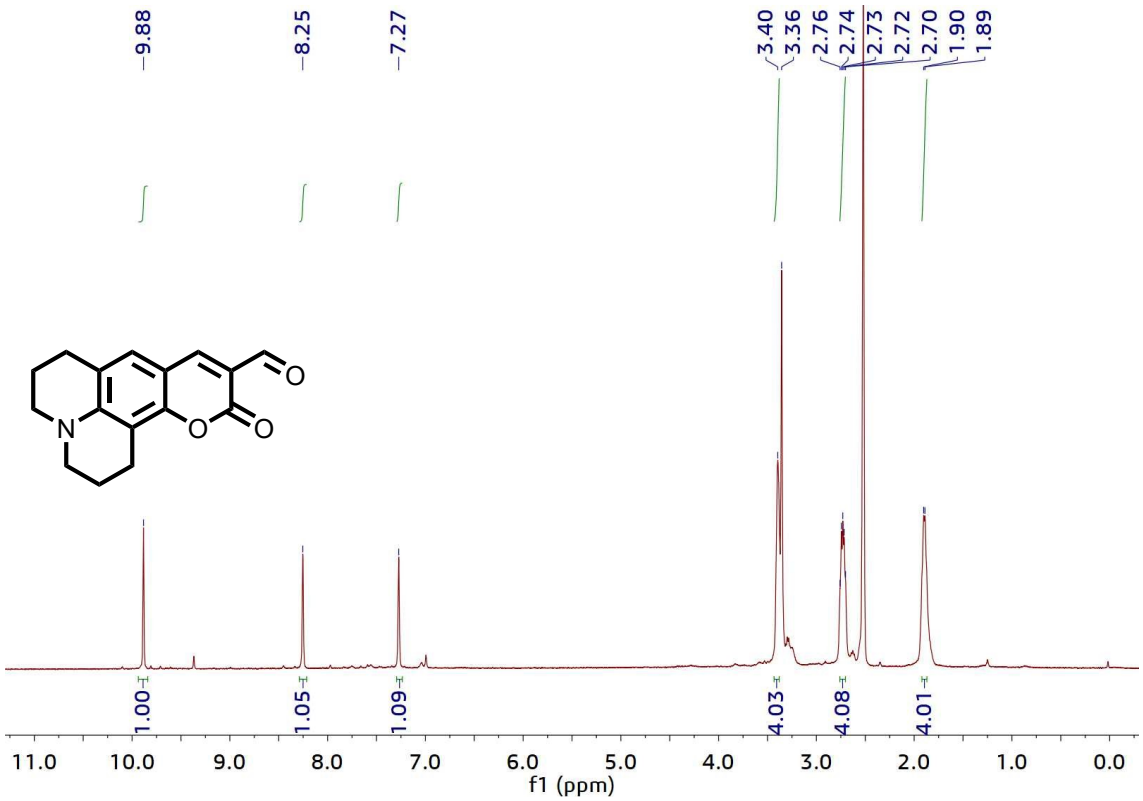

Fig. S13. ^{1}H NMR spectrum of 4c in DMSO-d_6.

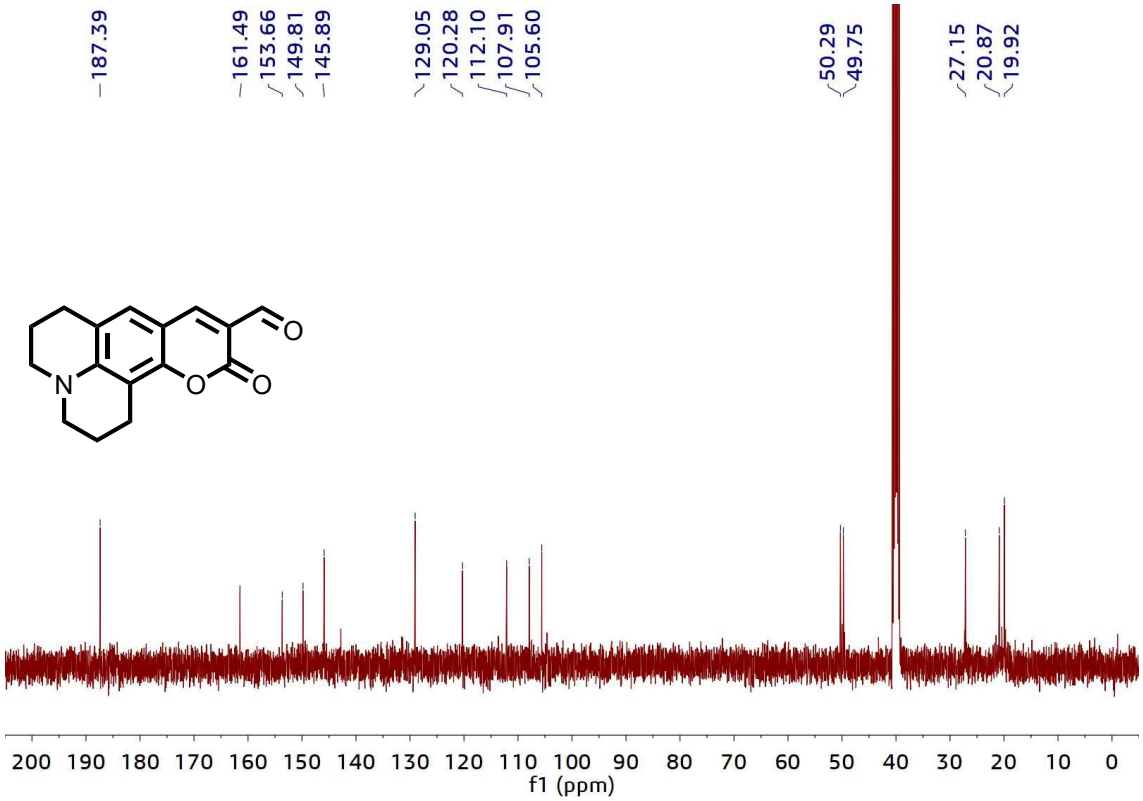

Fig. S14. ^{13}C NMR spectrum of 4c in DMSO-d_6.

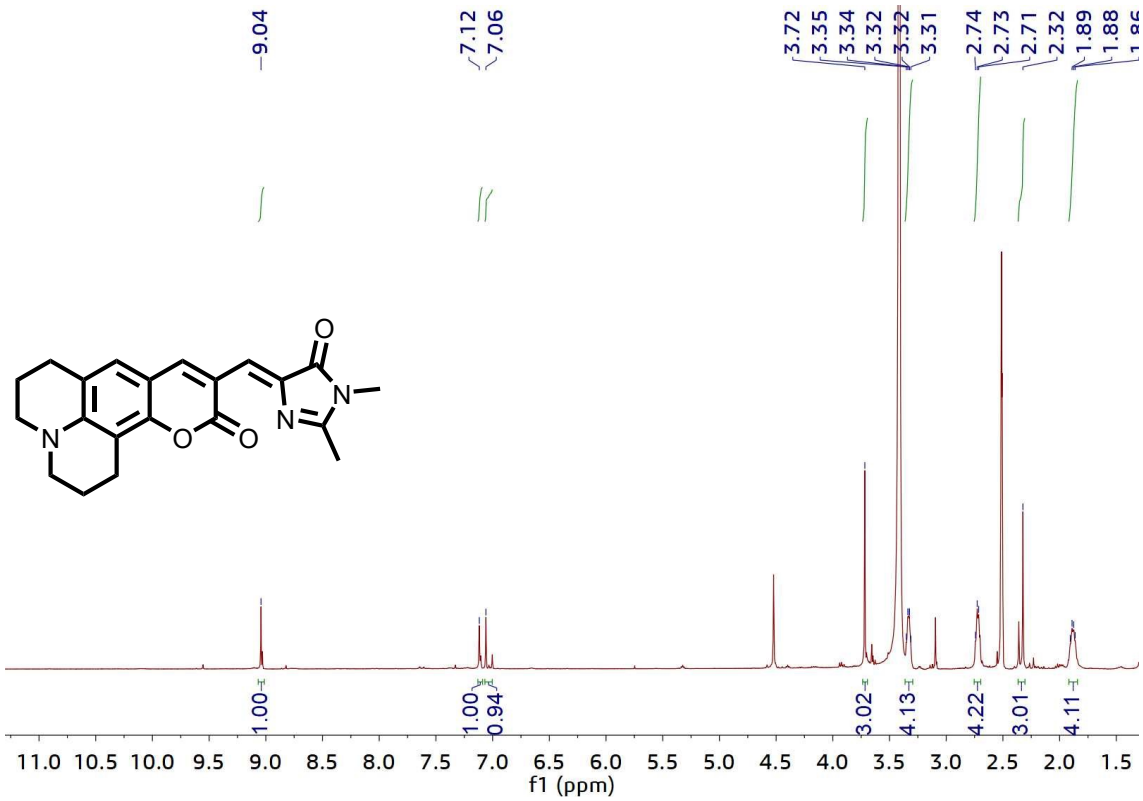

Fig. S15. ^{1}H NMR spectrum of NHCouI in DMSO-d_6.

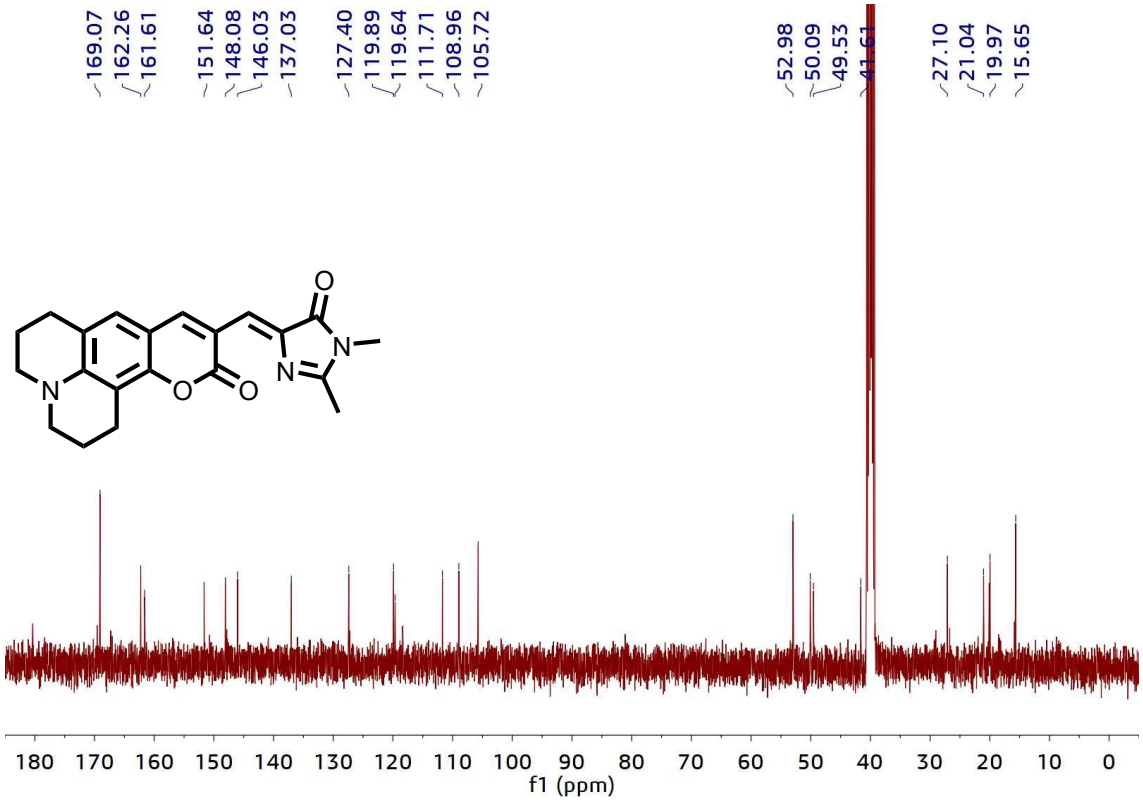

Fig. S16. ^{13}C NMR spectrum of NHCouI in DMSO-d_6.

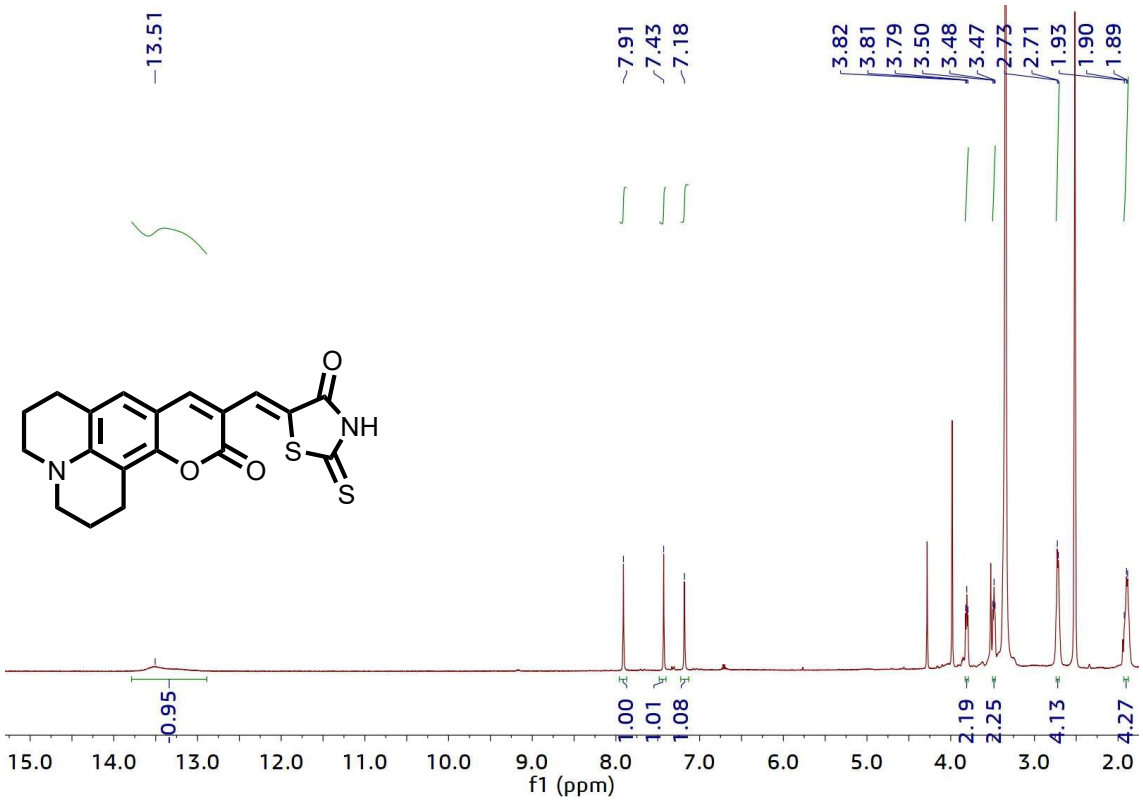

Fig. S17. [1]H NMR spectrum of NHCouR in DMSO-d_6.

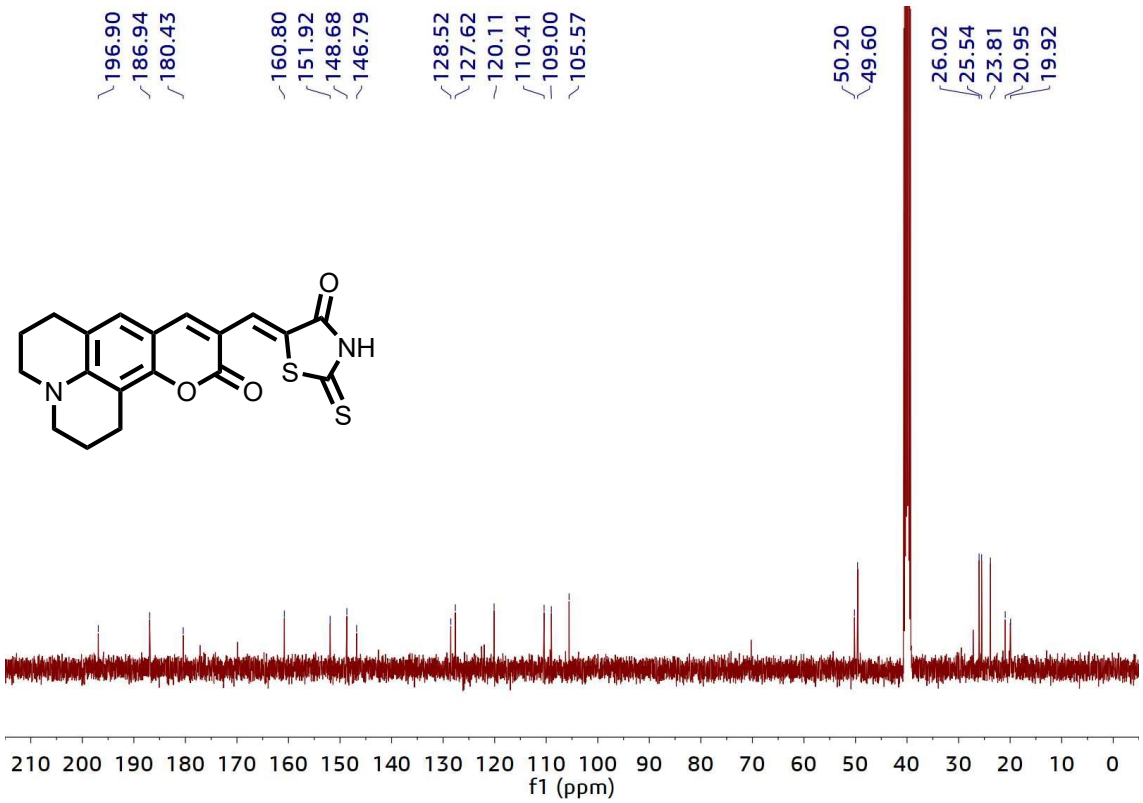

Fig. S18. [13]C NMR spectrum of NHCouR in DMSO-d_6.

4. Supporting discussion

The introduction of both the naphthalene ring and coumarin in the HBI backbone can expand the conjugation plane of the probe, which is beneficial to increase the π-π stacking of the probe with the G-quartet. As shown in Table S1, the G4 probe with a coumarin structure to G4s had higher binding affinity compared to the G4 probe with a naphthalene ring. In addition, it has been reported that G4 can bind to the rigid biscoumarin through hydrogen bonds and π-π interactions (|Chem. Commun., 2020, 56, 6870-6873). We speculate that the carbonyl oxygen group in the coumarin can have additional interactions with bases of G4s to improve the probe binding affinity.

Table S1. the dissociation constant (K_d) for dyes with the G4 structures.

Dye	G4 sequence	K_d (μM)	References
Ligand 1	22AG	5.5	J. Photochem. Photobiol. B, Biol. **2019,** 190, 128-136
Ligand 2	22AG	5.01	
QUMA-1	TERRA	0.57	Angew. Chem. Int. Ed. **2018**, 130, 4702-4706
CQ4	c-MYC Pu22	0.14	Angew.Chem.Int.Ed. **2020**,59,896–902
2c	c-MYC Pu22	0.30	ACS Chem. Biol. **2021**, 16, 1365−1376

5. Supplemental Figures and Tables

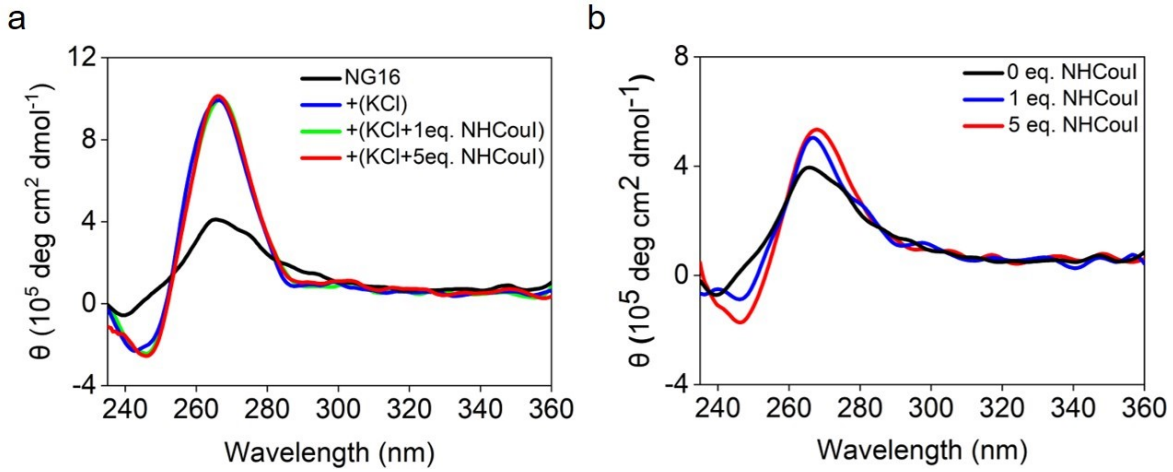

Fig. S19. (a) CD spectra of NG16 (10 μM) upon the addition of different equivalents of NHCouI in pH = 7.4, 25 mM Tris-HCl buffer with or without 100 mM KCl. (b) CD spectra of NG16 (10 μM) with different equivalents of NHCouI in pH = 7.4, 25 mM Tris-HCl buffer.

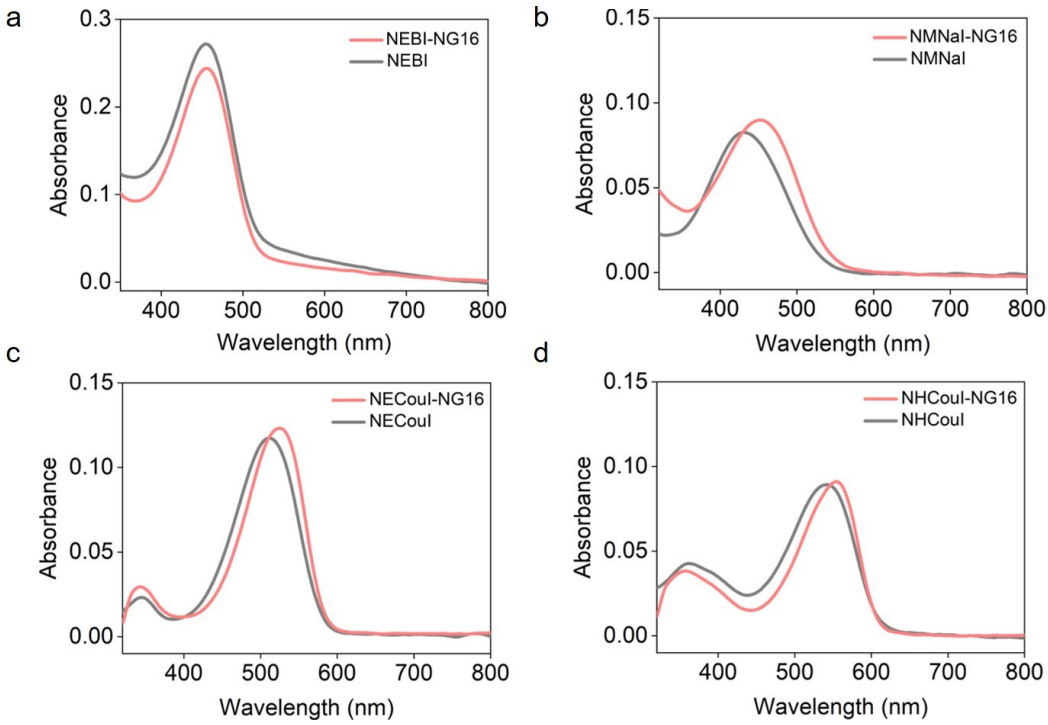

Fig. S20. Absorption spectra of (a) NEBI (5 μM), (b) NMNaI (5 μM), (c) NECouI (5 μM), (d) NHCouI (5 μM) before and after the addition of NG16 (25 μM) in Tris-HCl buffer (pH 7.4, 25 mM Tris, 100 mM KCl). (The red line represented the absorption of the chromophore alone, and the grey line represented the absorption of the chromophore after adding NG16).

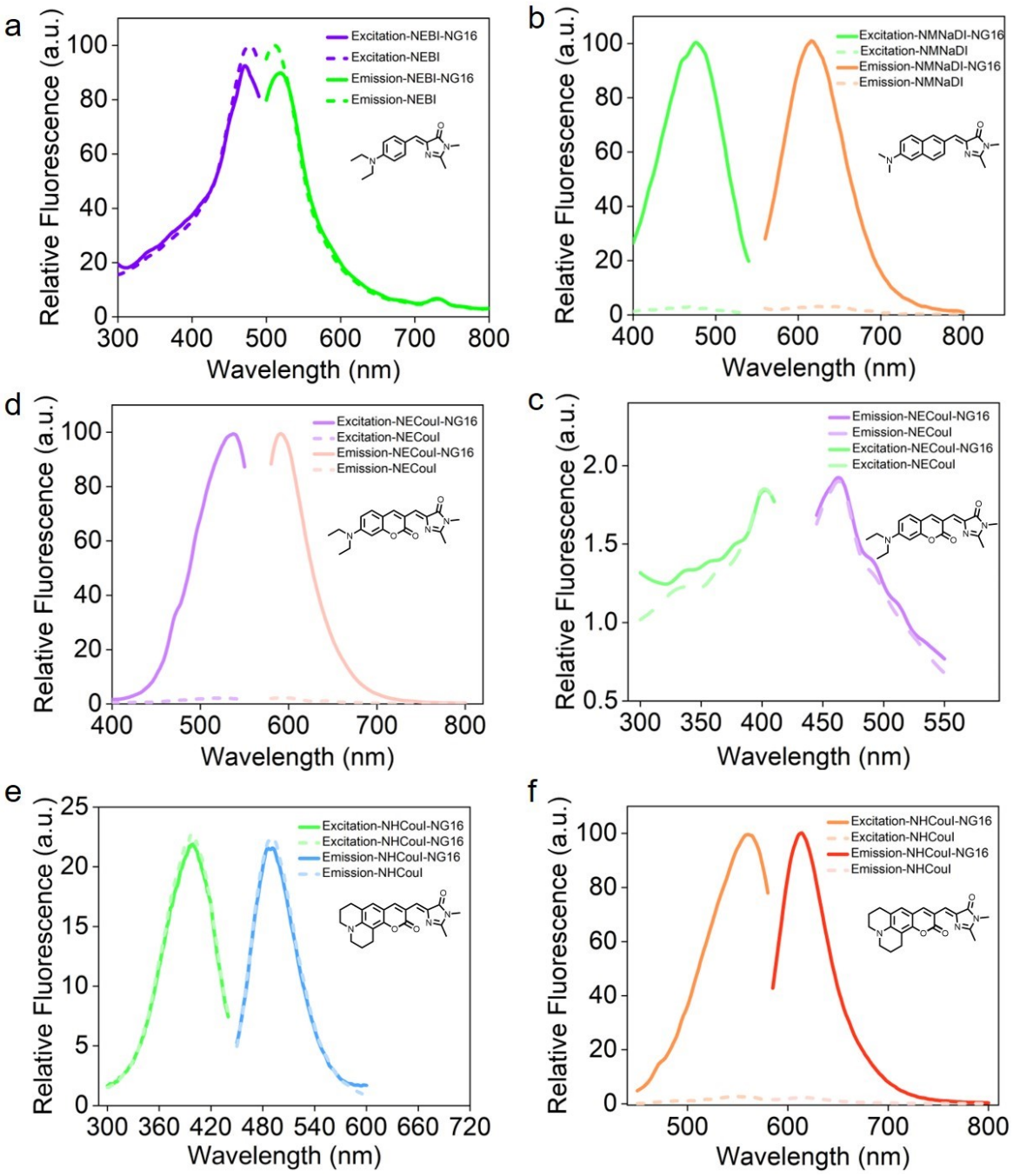

Fig. S21. Relative excitation and emission spectra of the chromophore (1 μM) before and after the addition of NG16 (5 μM) in Tris-HCl buffer (pH 7.4, 25 mM Tris, 100 mM KCl). (a) NEBI, (b) NMNaI, (c), (d) NECouI (e), (f) NHCouI. The dotted line represented the excitation and emission of the chromophore alone. The solid line represented the excitation and emission of the chromophore after adding NG16.

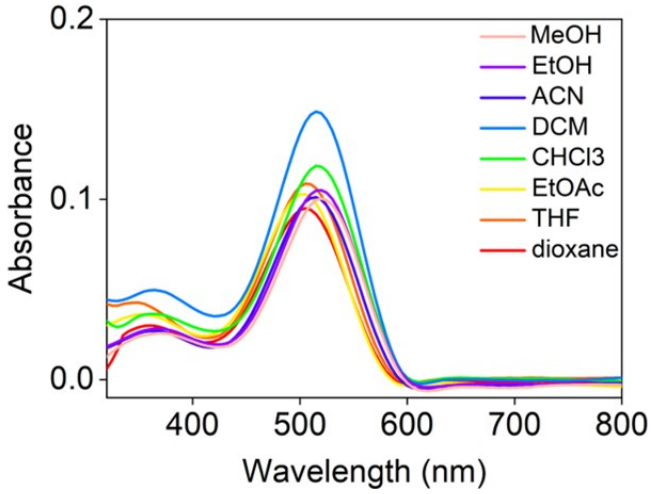

Fig. S22. The solvation effects on absorption of NHCouI (5 μM) in different solvents of different polarities.

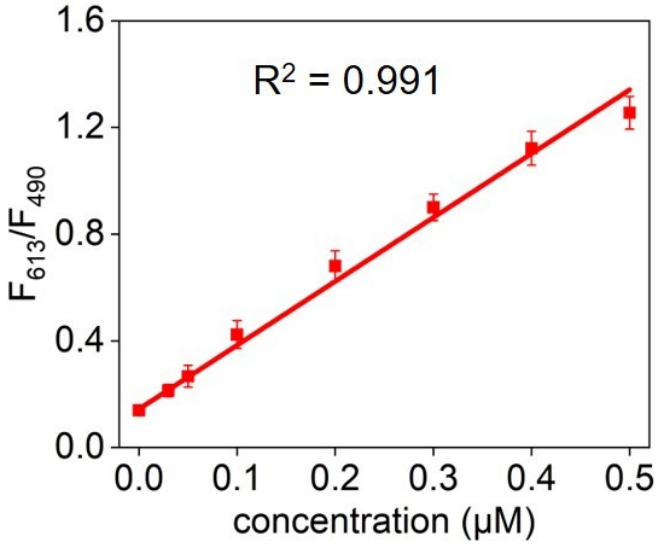

Fig. S23. Calibration curve of NHCouI-based assay for the detection of NG16 (0.03-0.5 μM) in Tris-HCl buffer (pH 7.4, 25 mM Tris, 100 mM KCl). NHCouI, 1 μM. LOD = 0.0168 μM.

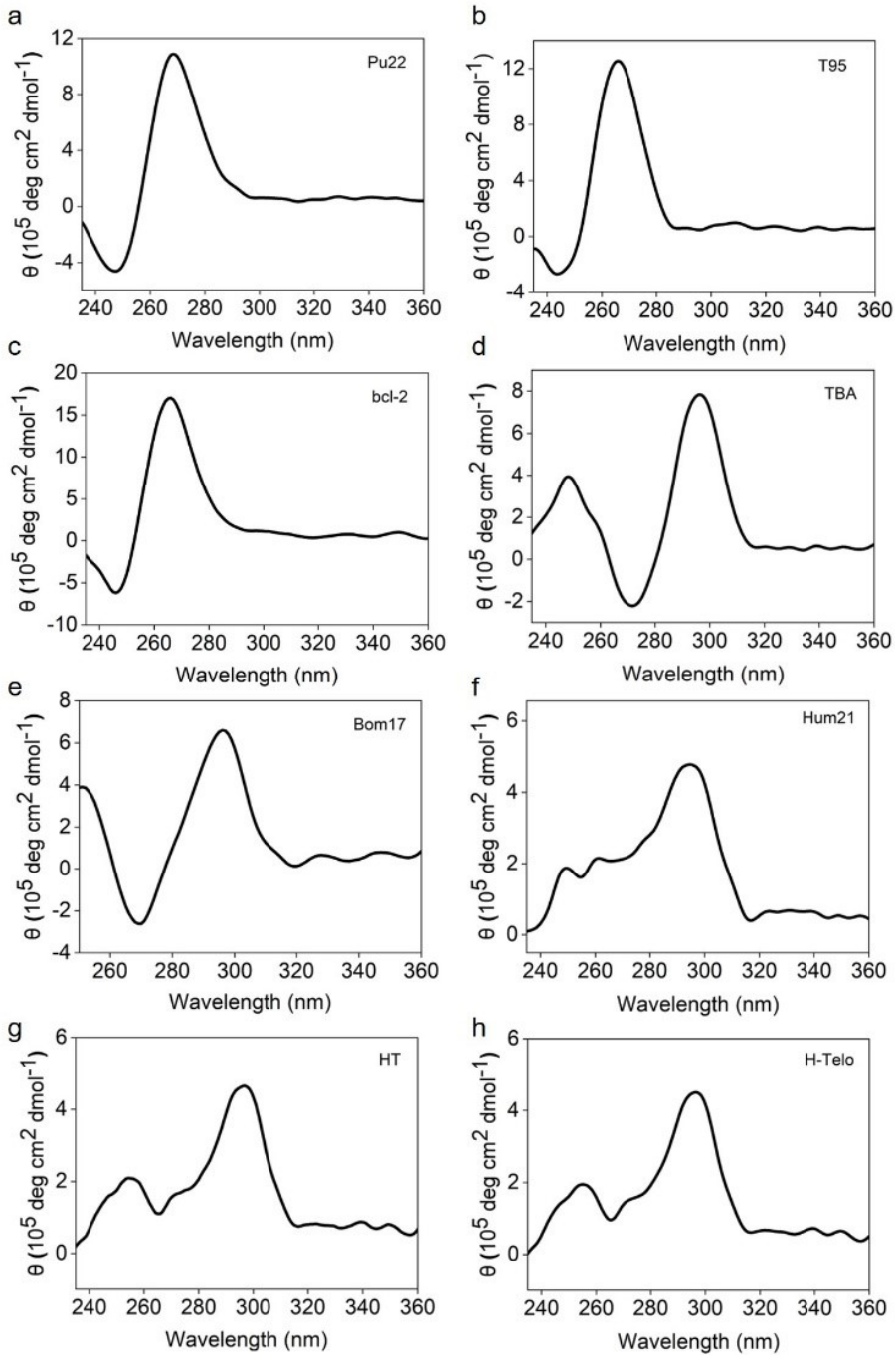

Fig. S24. CD spectra of various G4 oligonucleotides in Tris-HCl buffer (pH 7.4, 25 mM Tris-HCl, 100 mM KCl). (a) Pu22, (b) T95, (c) bcl-2, (d) TBA, (e) Bom17, (f) Hum21, (g) HT, and (h) H-Telo. Concentration of G4 oligonucleotides were 10 μM.

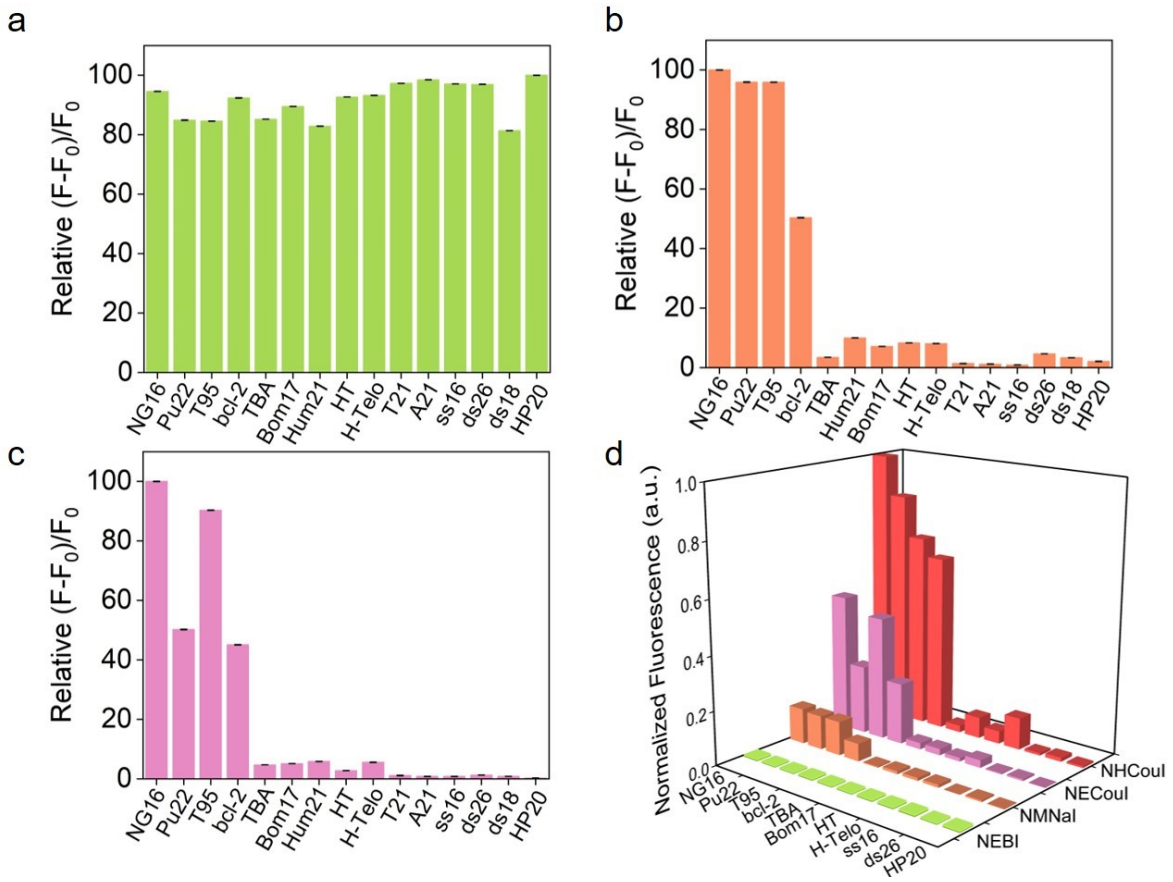

Fig. S25. Relative fluorescence intensity of (a) NEBI, (b) NMNaI, and (c) NECouI in response to different oligonucleotides (5 μM), including parallel G4s (NG16, Pu22, T95, and bcl-2), antiparallel G4s (TBA and Bom17), hybrid G4s (Hum21, HT and H-Telo), single-stranded oligonucleotides (T21, A21, and ss16), double-stranded oligonucleotides (ds26 and ds18) and hairpin (HP20). (d) Normalized fluorescence intensity of NEBI, NMNaI, NECouI, and NHCouI in response to different oligonucleotides (5 μM).

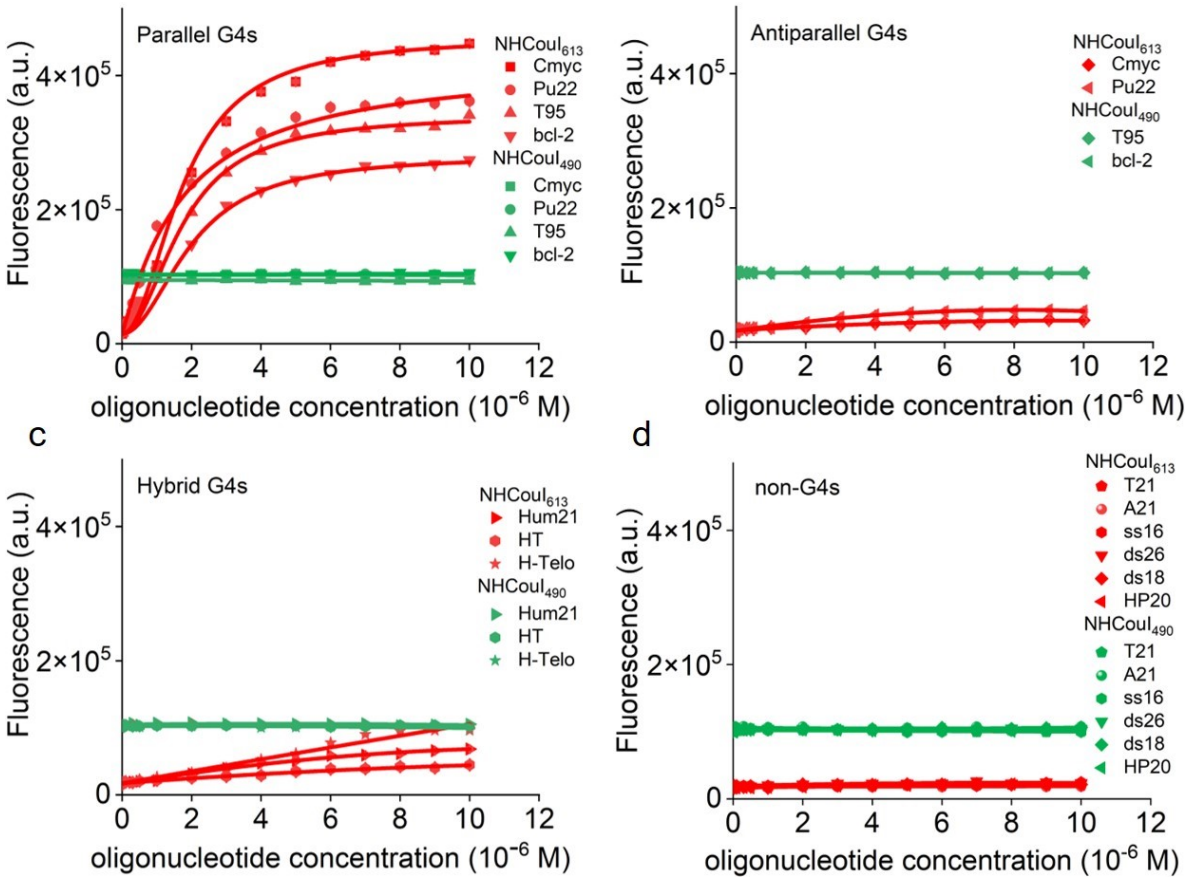

Fig. S26. Titration curves of fluorescence intensity of **NHCouI** (1 μM) as a function of the concentration of (a) parallel G4s, (b) antiparallel G4s, (c) hybrid G4s and non-G4 structures, respectively.

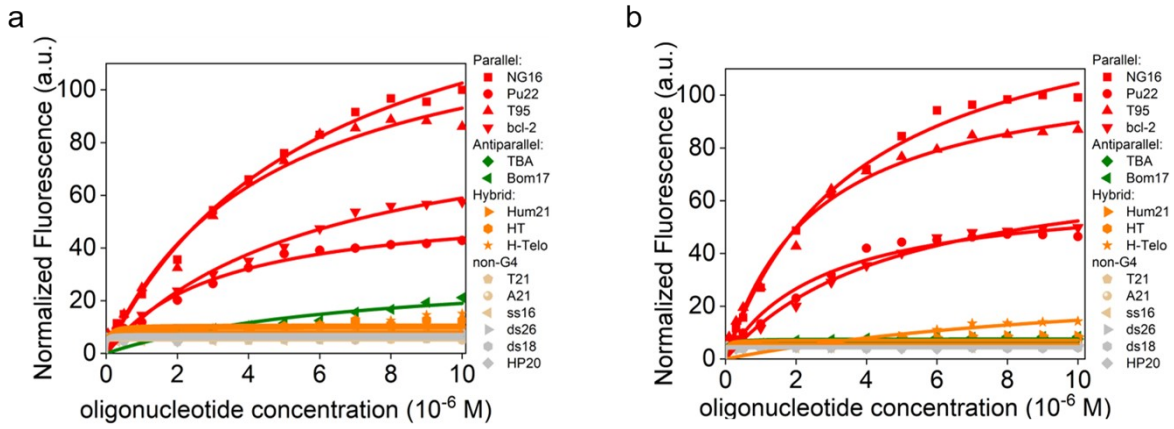

Fig. S27. Fluorescence titration curves of **NMNaI** (1 μM) and **NHCouI** (1 μM) as a function of different oligonucleotide concentration (0-10 μM), respectively.

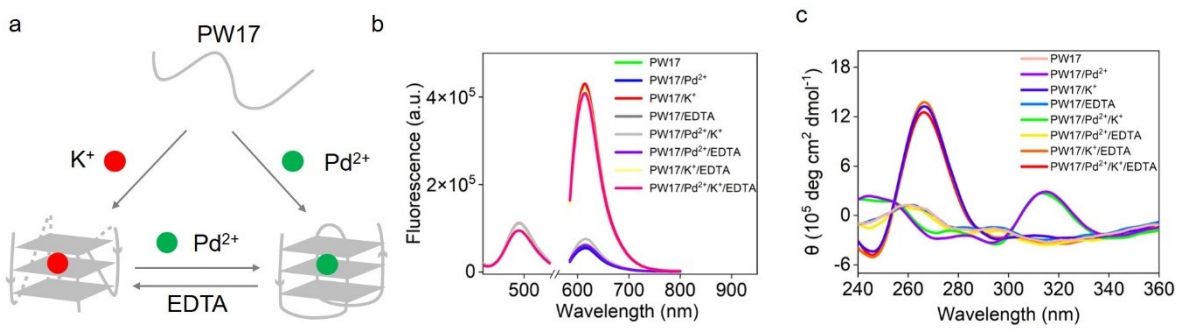

Fig. S28. (a) Schematic illustration of a topological switch based on the PW17-NHCouI, with K^+ 2 mM, Pb^{2+} 250 μM, and EDTA 250 μM. In the presence of K^+, the PW17 conformation is parallel; after adding Pd^{2+}, the PW17 conformation is antiparallel, then the introduction of EDTA, a Pb^{2+} chelator, leads to the re-formation of the parallel conformation of PW17. (b) Emission spectra at 490 nm and 613 nm of NHCouI in different conditions. (c) CD spectra of the PW17-NHCouI in different input conditions.

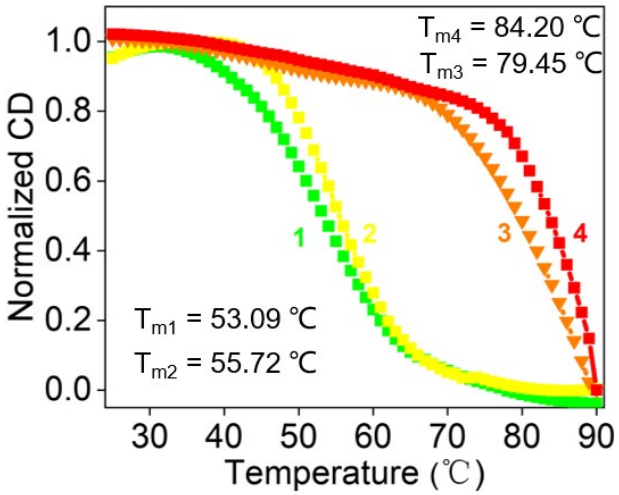

Fig. S29. CD melting curves of NG16 (10 μM) at 265 nm under different conditions. NG16 (curve1) and NG16 with NHCouI (20 μM, curve 2) in pH = 7.4, 25 mM Tris-HCl buffer without KCl; NG16 (curve 3) and NG16 with NHCouI (20 μM, curve 4) in pH = 7.4, 25 mM Tris-HCl buffer containing 100 mM KCl ($\Delta T_{m1\text{-}2}$ =2.63 ℃, $\Delta T_{m3\text{-}4}$ = 4.75 ℃).

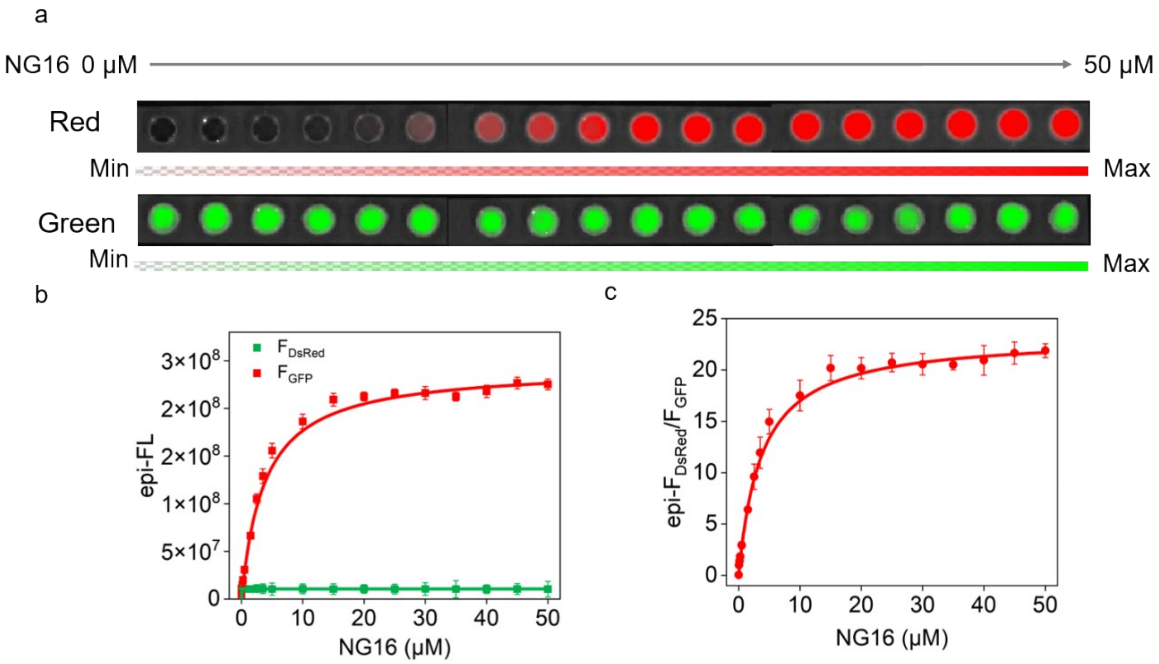

Fig. S30. Two-color visualization of NHCouI versus the concentration of NG16. (a) Two-color fluorescence visualization of NHCouI (5 μM) at different concentration of NG16 (0-10 equivalent) (λ_{ex} = 430 nm, received channel was GFP channel; λ_{ex} = 535 nm, received channel was DsRed channel;). (b) The fluorescence intensity of DsRed and GFP channels of NHCouI (5 μM) at different concentration of NG16 (0-10 μM). (c) The visualized titration curve of the F_{613}/F_{490} ratio of NHCouI (5 μM) versus different concentration of NG16 (0-10 equivalent).

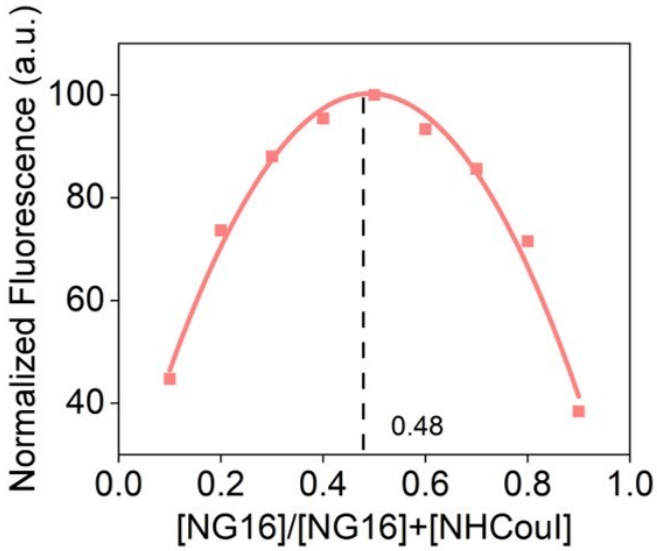

Fig. S31. Job's plot was obtained from fluorometric analysis of NHCouI-NG16 complex at 613 nm in pH = 7.4, 25 mM Tris-HCl buffer with 100 mM KCl. The total concentration of chromophore and NG16 is 3 μM.

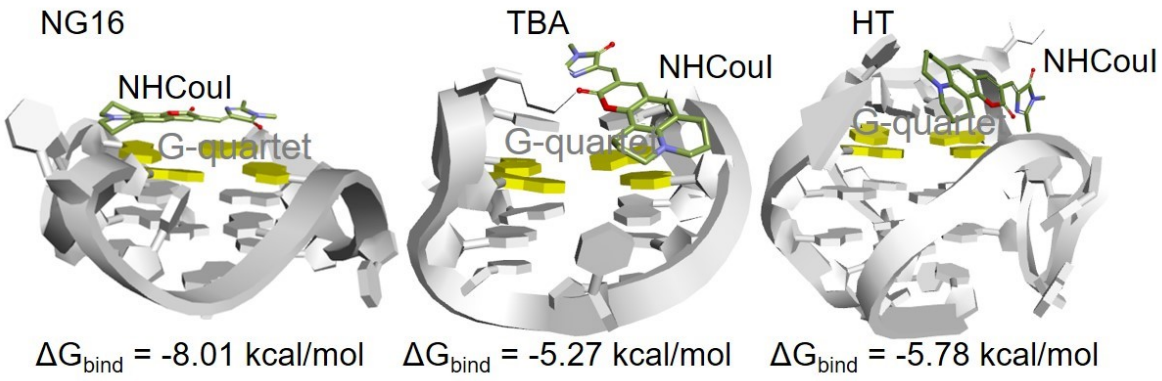

Fig. S32. Molecular docking results and free energies of NECouI with NG16, TBA, and HT, respectively.

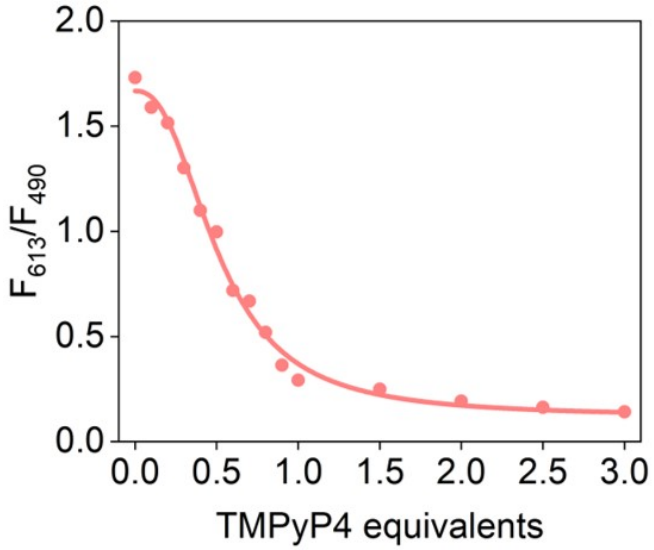

Fig. S33. F_{613}/F_{490} ratio of NHCouI-NG16 complex upon the addition of various amounts of TMPyP4 (0-15 μM) in pH = 7.4, 25 mM Tris-HCl buffer with 100 mM KCl. NHCouI, 5 μM; NG16, 5 μM.

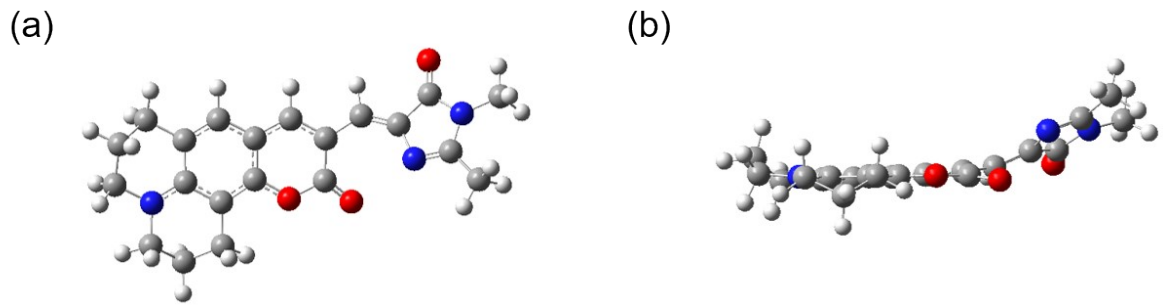

Fig. S34. Optimized geometry of **NHCouI** from (a) front view and (b) side view from DFT calculations in the ground state.

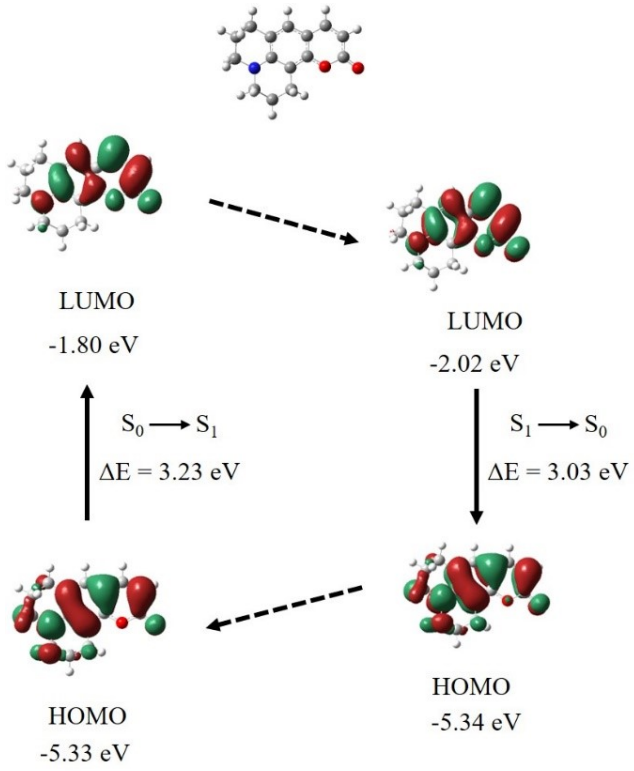

Fig. S35. Frontier molecular orbital plots of coumarin 6H in water involved in the vertical excitation (left) and emission (right). The vertical excitation-related calculations were based on the optimized geometry of the ground state (S_0), and the emission related-calculations were based on the optimized geometry of the excited state (S_1). Excitation and radiative processes are marked by solid lines, and the non-radiative processes are marked by dotted lines.

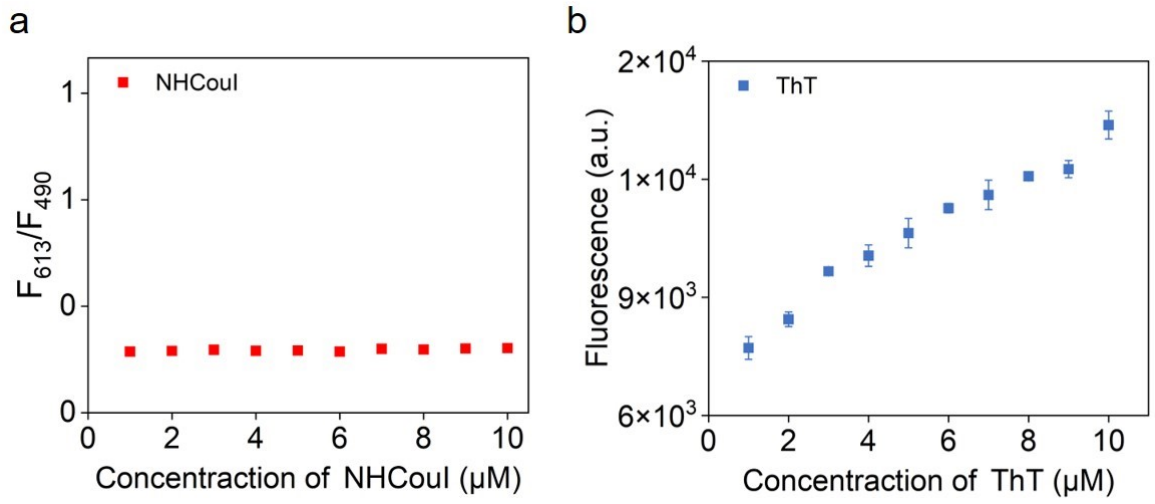

Fig. S36. (a) F_{613}/F_{490} ratio of NHCouI and (b) fluorescence intensity of ThT as a function of the dye concentration (1-10 μM).

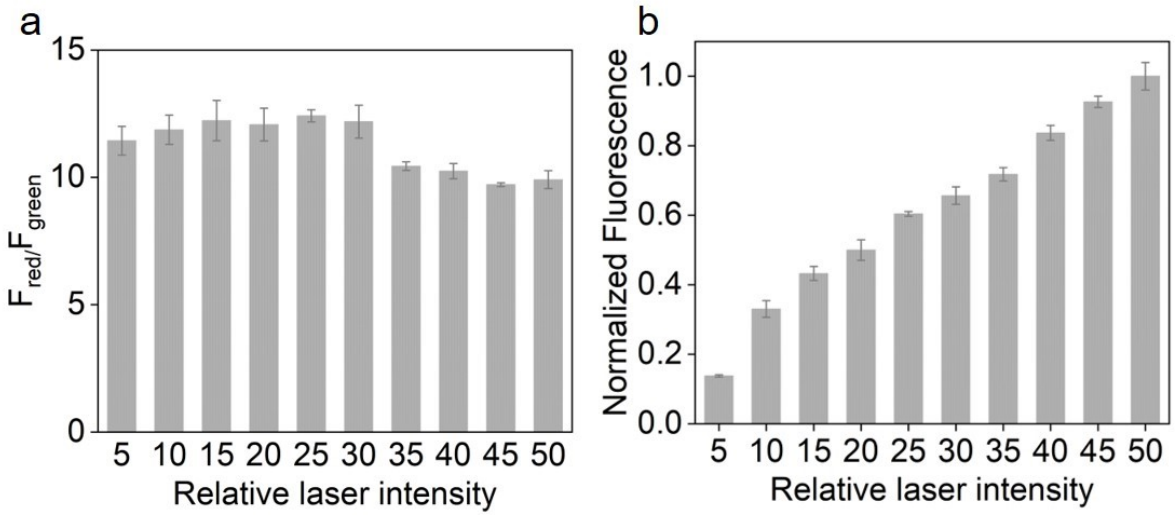

Fig. S37 (a) NHCouI's F_{red}/F_{green} ratio as a function of relative laser intensity. (b) Normalized fluorescence intensity of ThT as a function of relative laser intensity. Errors are S.D. (n = 3).

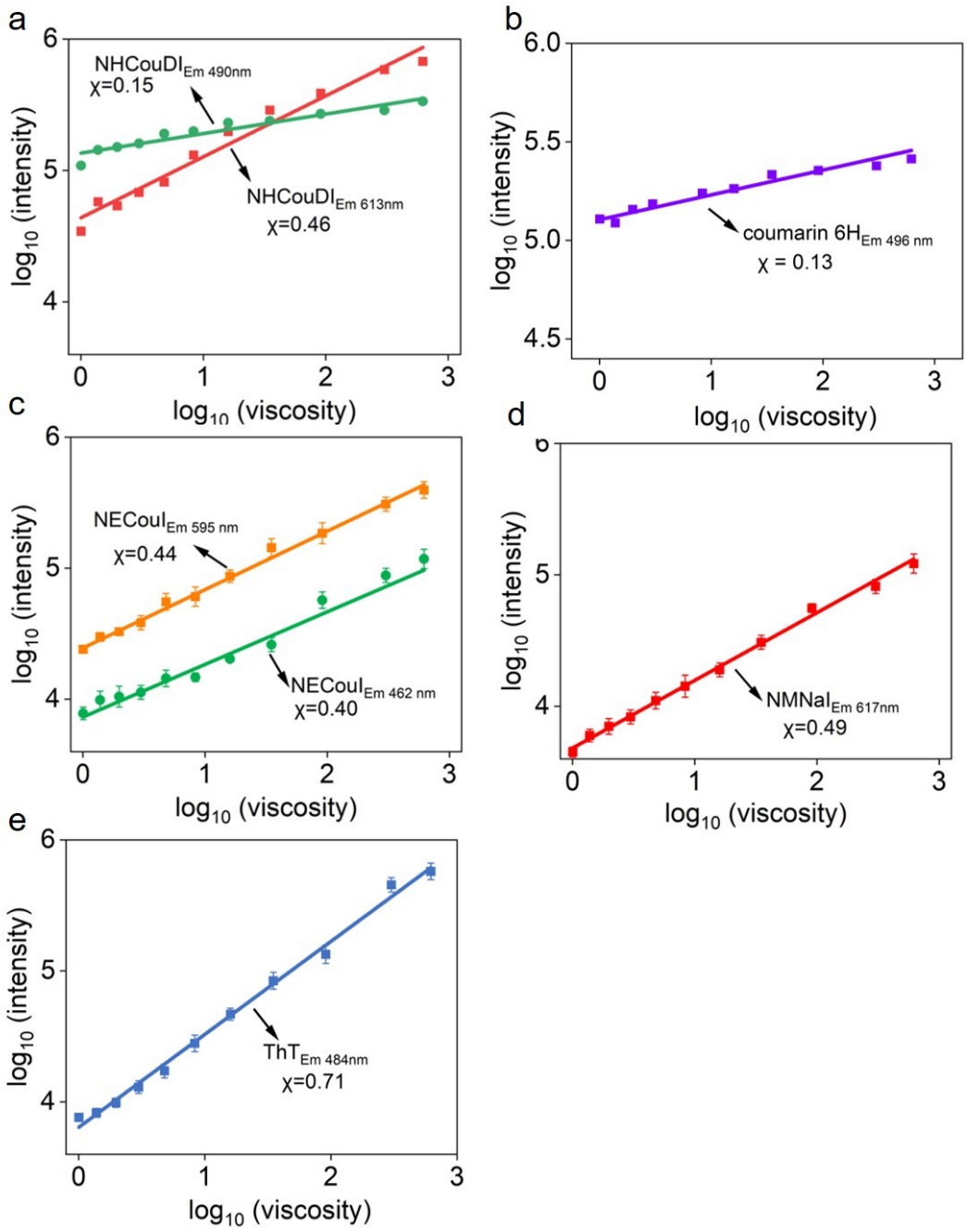

Fig. S38. Viscosity sensitivity calculated based on the fluorescence intensity of (a) NHCouI (λ_{em} = 490 nm and 613 nm), (b) coumarin 6H (λ_{em} = 496 nm), (c) NECouI (λ_{em} = 462 nm and 595 nm), (d) NMNaI (λ_{em} = 617 nm) and ThT (λ_{em} = 484 nm) in a mixture of water and glycerol, respectively.

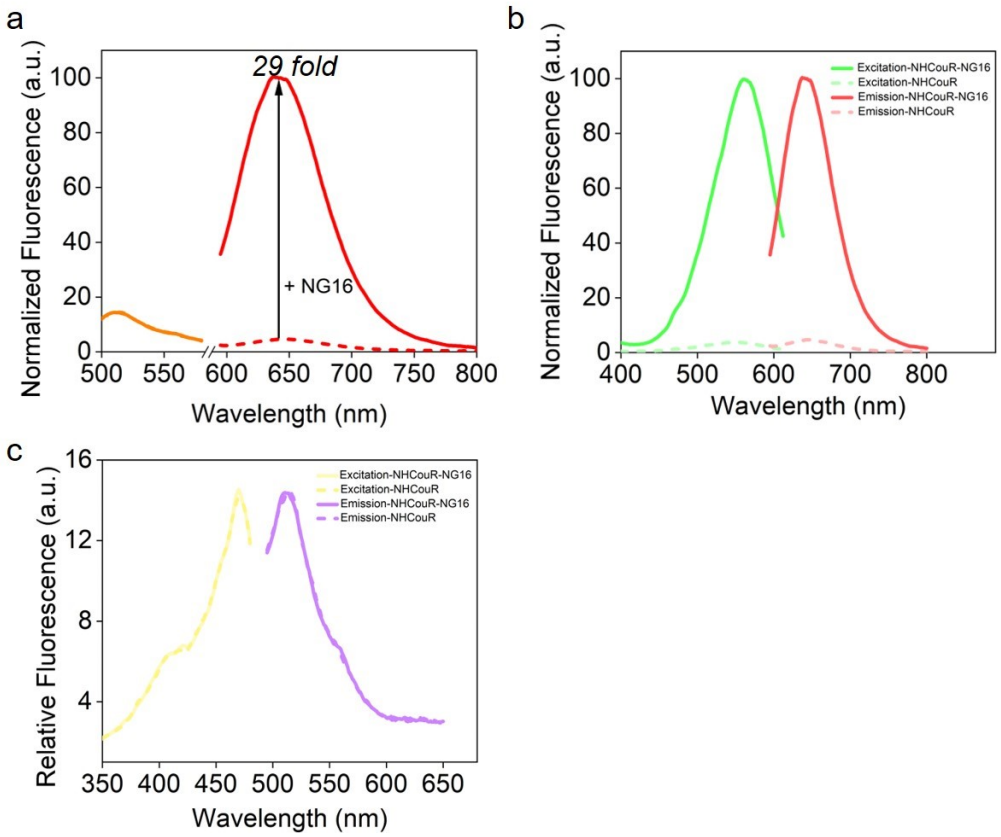

Fig S39. (a) The emission of NHCouR (1 μM) before and after the addition of NG16 (5 μM) (the dotted line was the emission of NHCouR alone, and the solid line is the emission of NHCouR after the addition of NG16. (b, c) Normalized and relative excitation and emission spectra of NHCouR (1 μM) before and after the addition of NG16 (5 μM) in Tris-HCl buffer (pH 7.4, 25 mM Tris, 100 mM KCl). The excitation and emission of (c) were the relative values of (b). The dotted line represented the excitation and emission of the NHCouR alone. The solid line represented the excitation and emission of the chromophore after adding NG16.

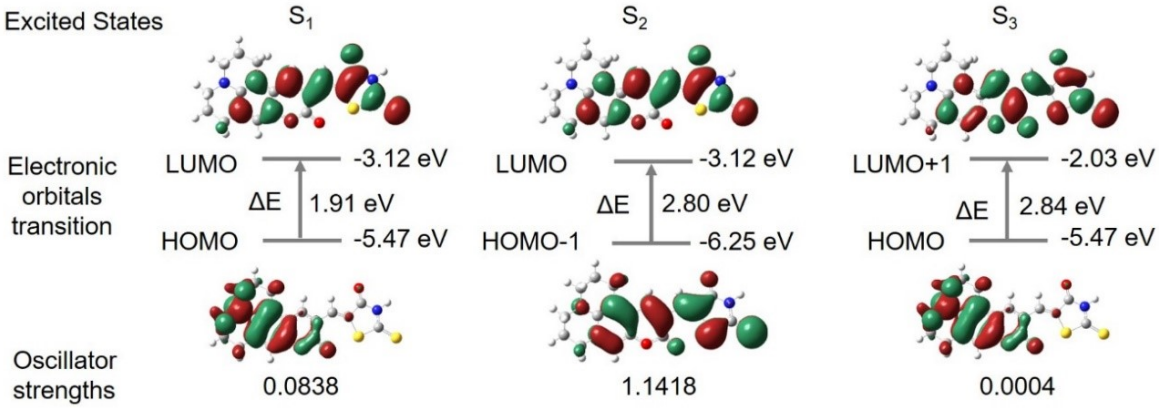

Fig. S40. The electronic orbital transitions, energy gaps, and oscillator strengths of NHCouR in the S_1, S_2, and S_3 excited states, were calculated by TDDFT at the B3LYP/6-31 + g(d) level.

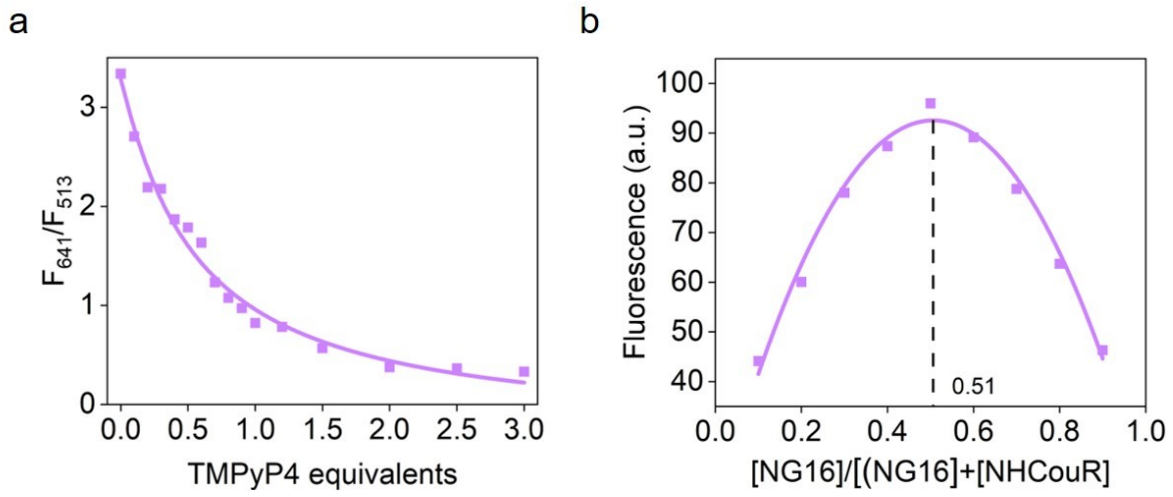

Fig. S41. (a) The F_{641}/F_{513} ratio of NHCouR-NG16 complex upon the addition of TMPyP4 (0-15μM) in pH = 7.4, 25 mM Tris-HCl buffer with 100 mM KCl. Chromophore, 5 μM; NG16, 5 μM. (b) Job's plot was obtained from fluorometric analysis of the NHCou- RD -NG16 complex at 641 nm in pH = 7.4, 25 mM Tris-HCl buffer with 100 mM KCl, respectively. The total concentration of NHCouR and NG16 is 3 μM.

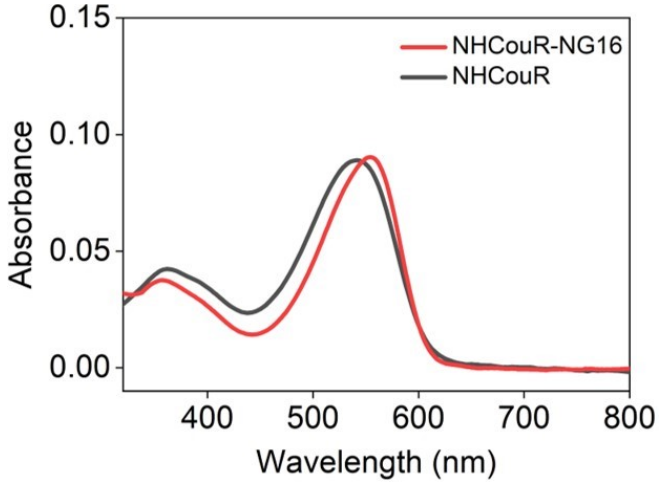

Fig. S42. Absorption spectra of the NHCouR (5 μM) before and after the addition of NG16 (25 μM) in Tris-HCl buffer (pH 7.4, 25 mM Tris, 100 mM KCl). The red line represented the absorption of the dye alone. The black line represented the emission of the probe after adding NG16).

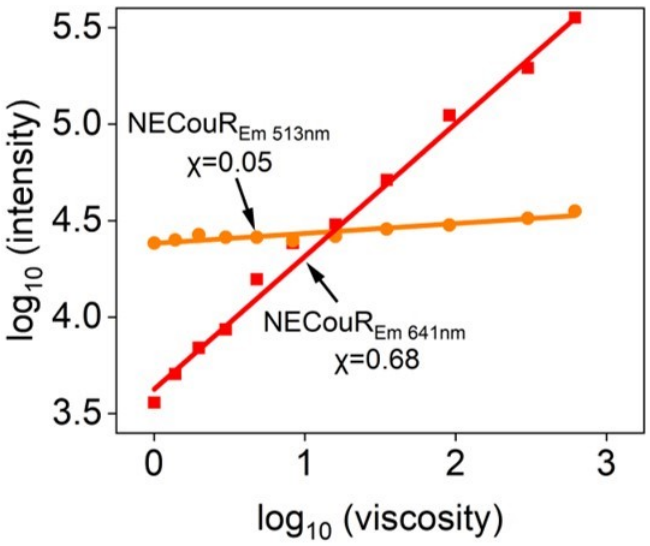

Fig. S43. Viscosity sensitivity calculated based on the fluorescence intensity of NHCouI (513 nm and 641 nm) in water and glycerol. Errors are S.D. (n = 3).

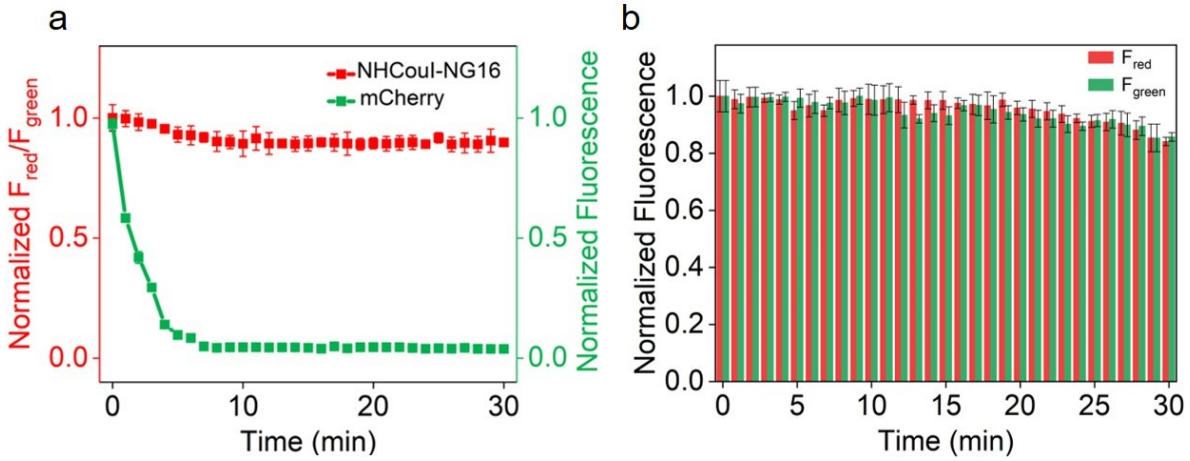

Fig. S44. (a) Photobleaching curves of NHCouI-NG16 (5 μM) and mCherry (5 μM), respectively. (b) Normalized fluorescence intensity of red and green channels of NHCouI as a function of laser irradiation time. Errors are S.D. (n = 3).

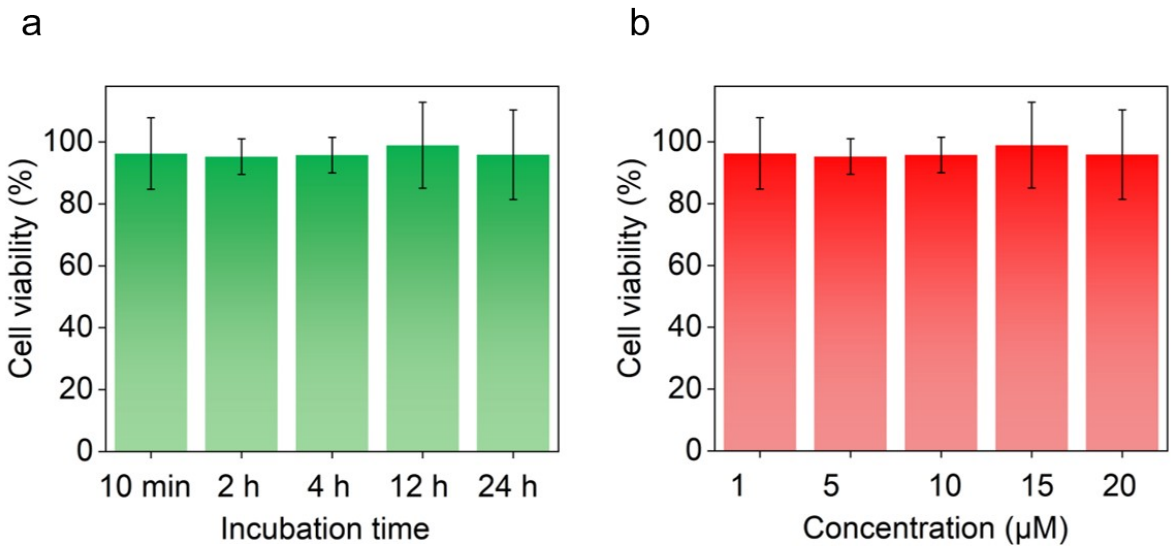

Fig. S45. The viability of HeLa cells in the presence of NHCouI was determined using the CCK8 assay. (a) HeLa cells were incubated with NHCouI (5 μM) at 37 °C with different incubation times (ranging from 10 mins to 24 h). (b) HeLa cells were incubated with NHCouI (1 to 20 μM) at 37 °C for 2 h. Data represent means ± SD, n = 5.

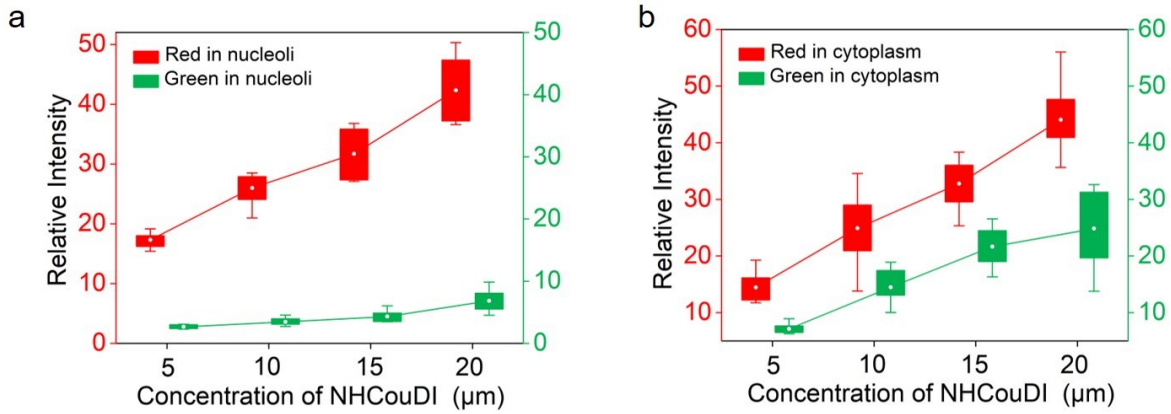

Fig. S46. The boxplots of the fluorescence intensities of both red and green channels in the (a) nucleoli and (b) cytoplasm of Figure 5a. Errors are S.D. (n = 10).

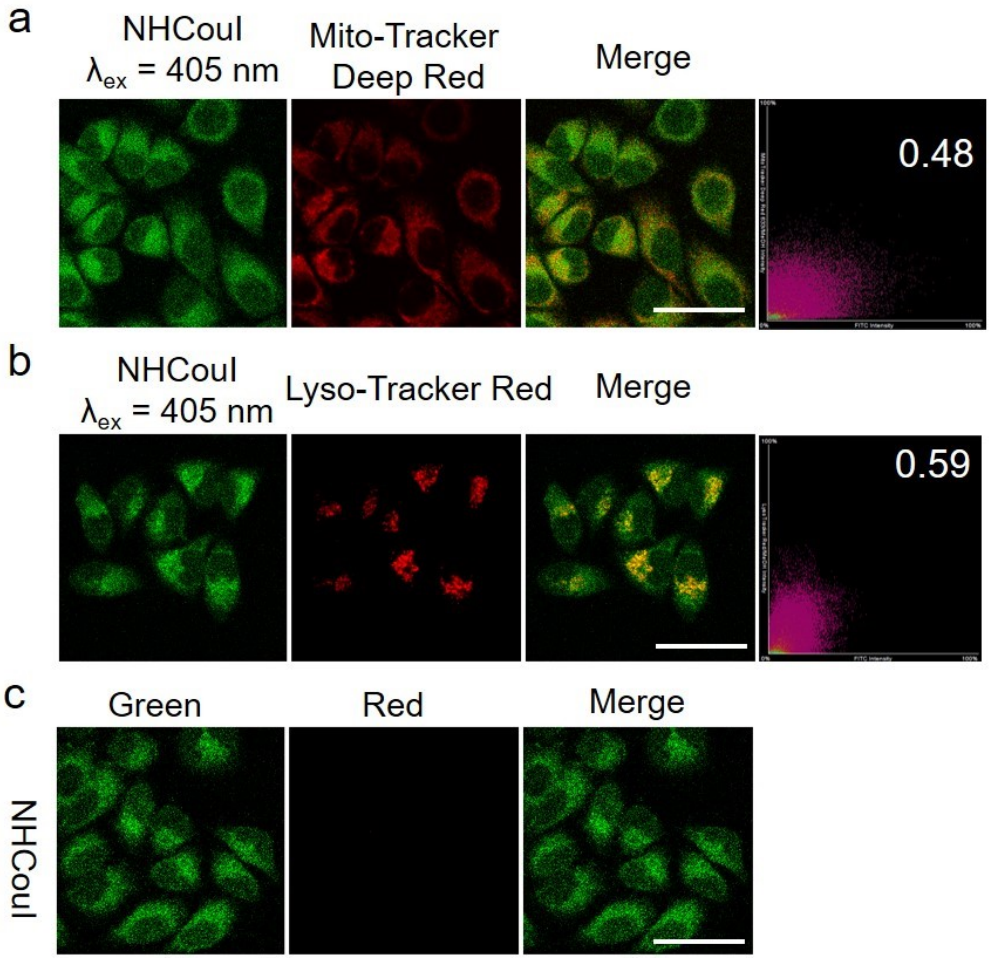

Fig. S47. Confocal imaging of living HeLa cells costained with 5 μM NHCouI (green) and different organelle trackers (red) for the mitochondria (a) and lysosome (b). (c) Verification of whether the red channel fluorescence of NHCouI is crosstalk with Lyso-Tracker Red. The red channel of NHCouI has no fluorescence under the laser condition that set the same to Lyso-Tracker Red. NHCouI (green): E_x/E_m 405/500-550 nm. Mito-Tracker Deep Red: 640/663-738 nm. Lyso-Tracker Red: E_x/E_m 561/570-620 nm. Scale bar: 50 μm.

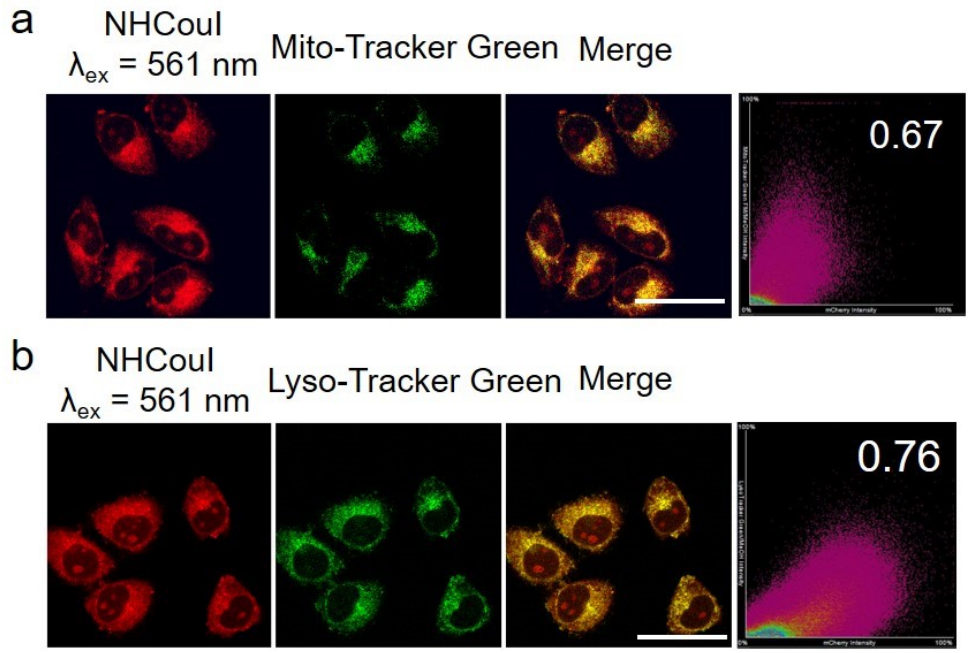

Fig. S48. Confocal imaging of living HeLa cells costained with 5 μM NHCouI (red) and different organelle trackers (green) for the mitochondria (a) and lysosome (b). NHCouI (red): E_x/E_m 561/570-620 nm. Mito-Tracker Green/Lyso-Tracker Green (green): E_x/E_m 488/500-550 nm. Scale bar: 50 μm.

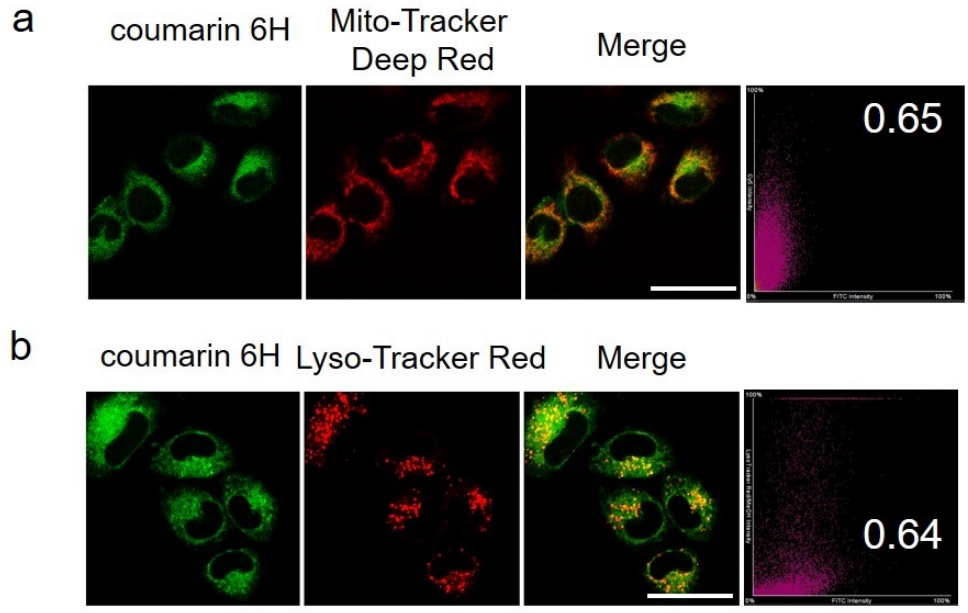

Fig. S49. Confocal imaging of living HeLa cells costained with 5 μM coumarin 6H (green) and different organelle trackers (red) for the mitochondria (a) and lysosome (b). coumarin 6H (green): E_x/E_m 405/500-550 nm. Mito-Tracker Deep Red: 640/663-738 nm. Lyso-Tracker Red: E_x/E_m 561/570-620 nm. Scale bar: 50 μm.

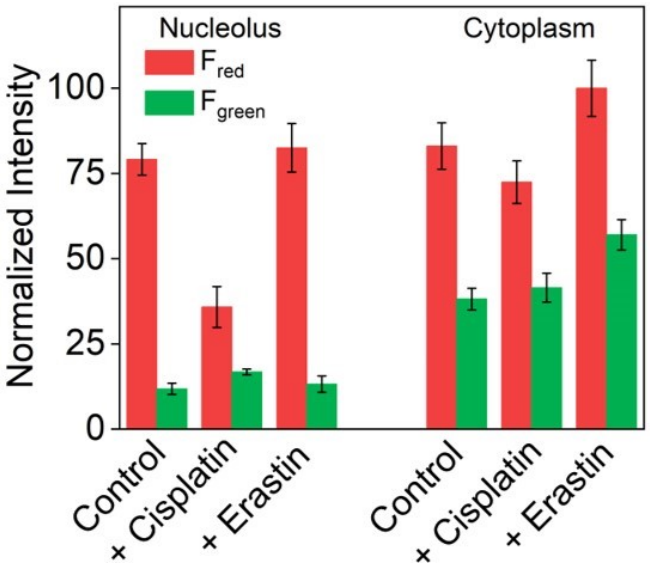

Fig. S50. Statistical plot of the fluorescence intensities of the red and green channels in the nucleoli and cytoplasm in live HeLa cells stained with 5 μM **NHCouI** for 120 min before and after the incubation with cisplatin (12.5 μM) or erastin (10 μM) for 12 h.

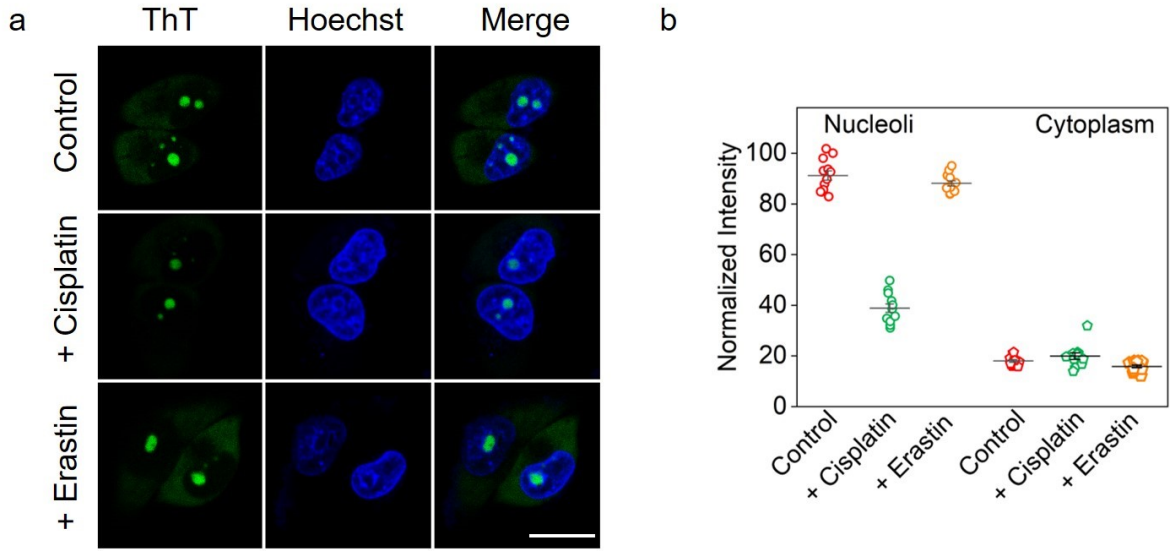

Fig. S51. (a) Fluorescent confocal imaging of live HeLa cells stained with 5 μM ThT for 120 min before and after the incubation with cisplatin (12.5 μM) or erastin (10 μM) for 12 h. (b) The normalized fluorescence intensity under different conditions. The images shown are representatives of replicate experiments. Errors are s. d. (n = 3). Scale bar = 20 μm.

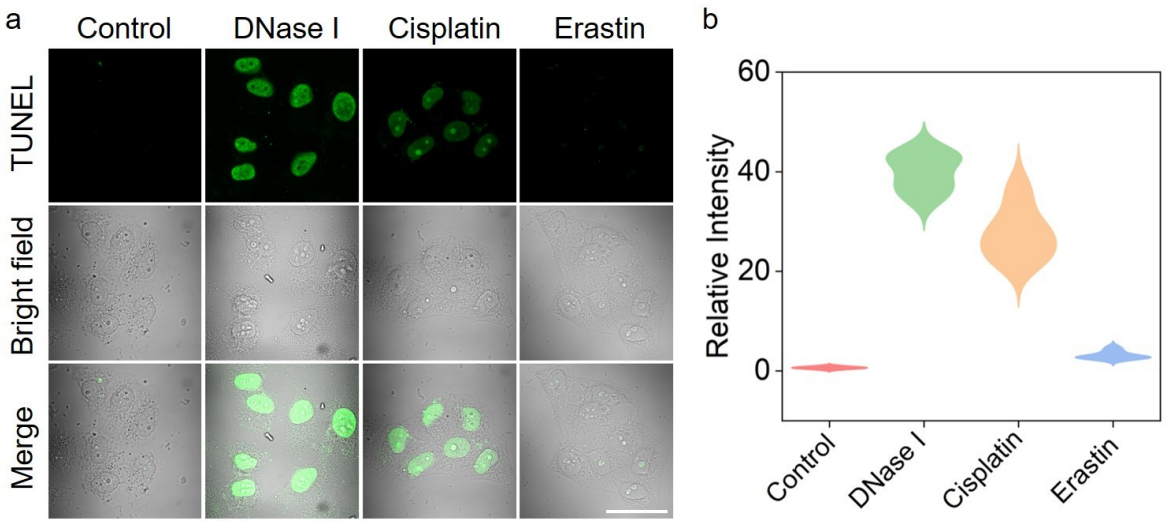

Fig. S52. Fluorescence confocal imaging of fixed HeLa cells was by using the TUNEL method before and after the treatment of DNase I (200 U) for 2 h、cisplatin (12.5 μM) for 24 h and erastin (10 μM) for 12 h. Scale bar = 50 μm.

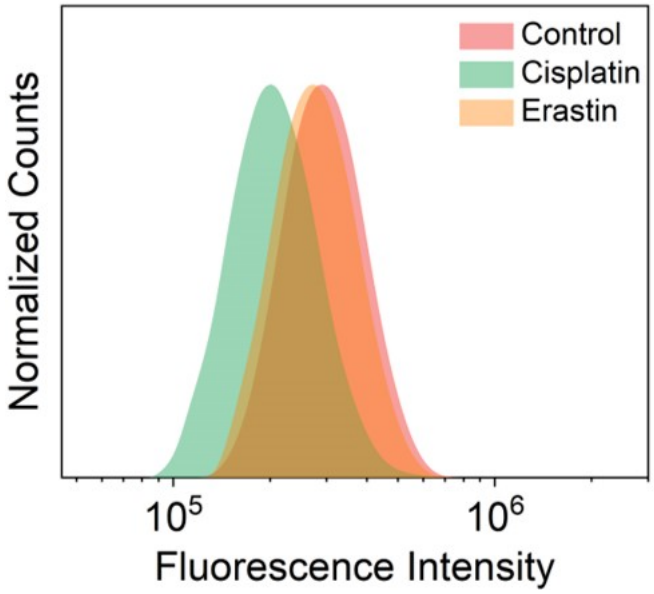

Fig. S53. Flow cytometric analysis of the Hela cells with or without the treatment of cisplatin (12.5 μM) or erastin (10 μM), respectively. The cell suspensions were stained with PI for 30 min at 37°C.

Table S2. Photophysical and binding properties of chromophores and chromophore-NG16 complexes.

Compound	λ_{ex} (nm)	λ_{em} (nm)	ε $(M^{-1}.cm^{-1})$	Stokes shift (nm)	Q.Y. [a]	K_d (μM)
HBI	418	490	51324	72	0.0014	N/A
HBI-NG16	420	490	50768	70	0.0007	N/A
Aequorea GFP[b]	395	508	27600	113	0.79	N/A
NEBI-NG16	455	522	48900	67	0.0074	N/A
NEBI	454	519	54400	65	0.0062	N/A
NMNaI-NG16	470	617	18100	147	0.18	2.79±0.12
NMNaI	468	630	16500	162	0.0064	N/A
NECouI-NG16	399 530	462 595	5820 24700	63 65	0.000016 0.47	1.37±0.18
NECouI	399 529	462 597	4700 33600	63 68	0.000019 0.0098	N/A
NHCouI-NG16	399 560	490 613	7650 18000	91 53	0.42, 0.62	1.48±0.15
NHCouI	399 563	490 615	8520 17900	91 52	0.38 0.012	N/A
NHCouR-NG16	471 565	513 641	7580 18100	42 76	0.077 0.25	1.67±0.25
NHCouR	471 566	513 647	8520 17800	42 81	0.069 0.0086	N/A

[a]Quantum yields were calculated using rhodamine 6G (Φ_F = 0.95 in water) as standard for chromophores. [b]See reference 9.

Table S3. Sequences and secondary structures of the oligonucleotides employed in this study.

Oligonucleotide	**Sequence (5'-3')**	**Structure type**
NG16	GGGTGGGTTGGGTGGG	Parallel G4
Pu22	TGAGGGTGGGTAGGGTGGGTAA	Parallel G4

T95	GGGTGGGTGGGTGGGT	Parallel G4
bcl-2	GGGCGGGCGCGGGAGGAAGGGGGCGGG	Parallel G4
TBA	GGTTGGTGTGGTTGG	Antiparallel G4
Bom17	GGTTAGGTTAGGTTAGG	Antiparallel G4
Hum21	GGGTTAGGGTTAGGGTTAGGG	Hybrid G4
HT	TTGGGTTAGGGTTAGGGTTAGGGA	Hybrid G4
H-Telo	GGGTTAGGGTTAGGGTTAGGG	Hybrid G4
T21	TTTTTTTTTTTTTTTTTTTT	Single strand
A21	AAAAAAAAAAAAAAAAAAAA	Single strand
ss16	CAATTGTATATATTCG	Single strand
ds26	CAATCGGATCGAATTCGATCCGATTG	Double strand
ds18	CAGTACAGATCTGTACTG	Double strand
HP20	CGCGCGCGTTTTCGCGCGCG	Hairpin

Table S4. The dissociation constant (K_d) of NHCouI with parallel G4s.

	K_d (μM)			
Probe	NG16	Pu22	T95	bcl-2
NECouI	1.37±0.18	1.64±0.16	2.65±0.13	2.58±0.23
NHCouI	1.48±0.15	1.55±0.24	1.44±0.29	2.59±0.19

Table S5. Photophysical properties of NHCouI after binding different kinds of oligonucleotides.

Structure type	Oligonucleotide	λ_{ex} (nm)	λ_{em} (nm)	Stokes shift (nm)	Q.Y.
Parallel G4	Pu22	399	490	91	0.40
		560	613	53	0.55

Antiparallel G4	T95	399	490	91	0.41
		560	612	52	0.46
	bcl-2	399	488	89	0.39
		560	613	53	0.43
	TBA	399	490	91	0.40
		563	614	51	0.048
	Bom17	399	488	89	0.39
		563	615	52	0.080
Hybrid G4	Hum21	399	488	89	0.39
		563	613	50	0.078
	HT	399	490	91	0.40
		563	613	50	0.065
	H-Telo	399	490	91	0.41
		563	615	52	0.097
Single strand	T21	399	490	91	0.41
		563	615	52	0.040
	A21	399	490	91	0.41
		563	615	52	0.036
	ss16	399	490	91	0.40
		563	615	52	0.041
Double strand	ds26	399	490	91	0.41
		563	615	52	0.017
	ds18	399	490	91	0.40
		563	615	52	0.040
Hairpin	HP20	399	490	91	0.41
		563	615	52	0.037

Table S6. The optimized geometry of NHCouI at the ground state (S_0). The total energy at this geometry is -1202.9110557 Hartree. The geometry was optimized using Gaussian 09.

Atom Label	Atom	X(Å)	Y(Å)	Z(Å)
1	C	-5.95782100	-1.99020100	-0.71144800
2	C	-6.47331500	-0.78759400	0.07027800
3	N	-5.39528900	0.12139500	0.48507600
4	C	-4.08366700	-0.25200800	0.54045500
5	C	-3.71852900	-1.62931300	0.31640300
6	C	-4.80789100	-2.64428000	0.05743300
7	C	-5.83669100	1.48864100	0.78659600
8	C	-4.85762900	2.22145800	1.69448800
9	C	3.44541000	2.15292300	1.10859000
10	C	-3.07252400	0.71569100	0.82435000
11	C	-1.75333900	0.28882600	0.84344900
12	C	-1.36118400	-1.04623500	0.58929000
13	C	-2.39035300	-1.98668600	0.32962900
14	O	-0.78983100	1.22433400	1.12906400
15	C	0.57494100	0.95494100	1.18543900
16	C	0.99920700	-0.38040600	0.77312200
17	C	0.01517600	-1.34077700	0.56767800
18	O	1.27123200	1.85637300	1.62130600
19	C	2.38588300	-0.77525500	0.65153200
20	C	3.52067700	-0.08695600	0.34280800
21	N	3.69041200	1.25230700	-0.03785000
22	C	4.95663000	1.39158200	-0.31887100
23	N	5.70375900	0.22440400	-0.14945100
24	C	4.83825400	-0.77824200	0.27138000
25	O	5.15095800	-1.94828500	0.51241800

26	C	5.59260800	2.65503300	-0.78830500
27	C	7.13057000	0.04870400	-0.37361400
28	H	-6.78247400	-2.69462300	-0.86420400
29	H	-5.60948900	-1.66942700	-1.70173300
30	H	-7.02454000	-1.11889900	0.96340600
31	H	-7.17235700	-0.20600300	-0.54233600
32	H	-4.39920600	-3.49889000	-0.49263500
33	H	-5.19174500	-3.03642300	1.01147300
34	H	-6.82009500	1.41609400	1.26497800
35	H	-5.97453700	2.03984600	-0.15657000
36	H	-5.18265000	3.26135500	1.80576100
37	H	-4.86871200	1.76421900	2.69228000
38	H	-2.72063300	2.59856100	1.79637500
39	H	-3.40076300	2.74714600	0.18352900
40	H	-2.11350300	-3.02051000	0.13445300
41	H	0.32099500	-2.36204100	0.34809900
42	H	2.55181400	-1.84629900	0.76835100
43	H	4.83385700	3.43707500	-0.85673900
44	H	6.37889800	2.98266700	-0.09709300
45	H	6.05796600	2.52314800	-1.77278000
46	H	7.71171100	0.70636000	0.27953300
47	H	7.37349700	-0.98986200	-0.14200000
48	H	7.38943100	0.25243200	-1.41699100

Table S7. The optimized geometry of NHCouR at the ground state (S_0). The total energy at this geometry is -1865.3040315 Hartree. The geometry was optimized using Gaussian 09.

Atom Label	Atom	X(Å)	Y(Å)	Z(Å)

1	C	-3.97821800	-1.42374900	0.61029200
2	C	-3.91496500	-0.05180900	1.02053400
3	C	-2.72986700	0.68403500	0.80036200
4	C	-1.61440700	0.04392700	0.19035900
5	C	-1.71734600	-1.30376600	-0.20356500
6	C	-2.88327100	-2.02579300	-0.00386800
7	C	-5.21990300	-2.25577000	0.85596700
8	C	-6.45788600	-1.39189100	1.09788200
9	C	-6.12028100	-0.29419400	2.09991300
10	N	-5.03671100	0.55023300	1.59751400
11	C	-4.84843100	1.80716300	2.31809000
12	C	-3.99717000	2.76418500	1.49414400
13	C	-2.62692000	2.14186600	1.21156900
14	O	-0.35958400	0.67477100	-0.04603500
15	C	0.71104200	0.02614800	-0.63308100
16	C	0.55212000	-1.36770200	-1.04124500
17	O	-0.66097800	-1.95282200	-0.79825800
18	O	1.40330800	-2.06103200	-1.58173900
19	C	1.94092100	0.76221000	-0.81823600
20	C	3.17173800	0.47780900	-1.32123600
21	H	-2.93312300	-3.06423600	-0.31855500
22	H	-5.37522500	-2.94015100	0.01370000
23	H	-5.04431900	-2.89107700	1.73698100
24	H	-7.28172600	-2.00413800	1.48046200
25	H	-6.79449200	-0.93379400	0.15913900
26	H	-5.85133600	-0.74159700	3.07411100
27	H	-6.98741000	0.35245400	2.26849700

28	H	-4.37794700	1.62835400	3.30217200
29	H	-5.83876900	2.23515400	2.50344000
30	H	-3.87688400	3.71315700	2.02787900
31	H	-4.51588700	2.98011600	0.55165100
32	H	-1.99494500	2.22458200	2.10808700
33	H	-2.12466500	2.72295000	0.42979800
34	H	-0.22325400	1.70962600	0.25079300
35	H	1.87623200	1.79325400	-0.47129000
36	C	4.19011600	1.56281900	-1.32042900
37	O	4.05275000	2.71250000	-0.91958800
38	N	5.38223000	1.08373400	-1.85912600
39	H	6.19289200	1.69166500	-1.93772500
40	S	3.87793500	-1.000216 00	-2.01546300
41	C	5.43504800	-0.21442400	-2.27787400
42	S	6.76174000	-0.96066400	-2.94128100

6. References

1. L. Zhang, J. C. Er, K. K. Ghosh, W. J. Chung, J. Yoo, W. Xu, W. Zhao, A. T. Phan, Y. T. *Chang. Sci. Rep.* 2014, **4**, 3776–3781.

2. Wurth, C.; Gonzalez, M. G.; Niessner, R.; Panne, U.; Haisch, C.; Genger, U. R. *Talanta*，2012, *90*, 30–37.

3. V. Kuryavyi, L.A. Cahoon, H.S. Seifert, D. J. Patel. *Structure*, 2012, **20**, 2090–2102.

4. H.M. Berman, J. Westbrook, Z. Feng, G. Gilliland, T.N. Bhat, H. Weissig, I.N. Shindyalov, P.E. Bourne. *Nucleic Acids Res.*, 2000, **28**, 235–242.

5. G. M. Morris, R. Huey, W. Lindstrom, M. F. Sanner, R. K. Belew, D. S. Goodsell, A. J. Olson. *J. Comput. Chem.*, 2009, **30**, 2785–2791

6. K. N. Luu, A. T. Phan, V.V. Kuryavyi, L. Lacroix, D. J. Patel. *J. Am. Chem. Soc.*, 2006, *128*, 9963–9970.

7. J. Lietard, H. Abou Assi, I. Gomez-Pinto, C. Gonzalez, M. M. Somoza, M. J. Damha. *Nucleic Acids Res.*, 2017, **45**, 1619–1632.

8. T. D. Bergazin, N. Tielker, Y. Zhang, J. Mao, M. R. Gunner, K. Francisco, B. Carlo, M. K. Stefan, D. L. Mobley. *J. Comput. Aided Mol. Des.*, 2021, **35**, 771–802.

9. G. H. Patterson, S. M. Knobel, W. D. Sharif, S. R. Kain, D. W. Piston. *Biophys. J.* 1997, **73**, 2782-2790.